

UC San Diego

JACOBS SCHOOL OF ENGINEERING

Department of Mechanical and Aerospace Engineering



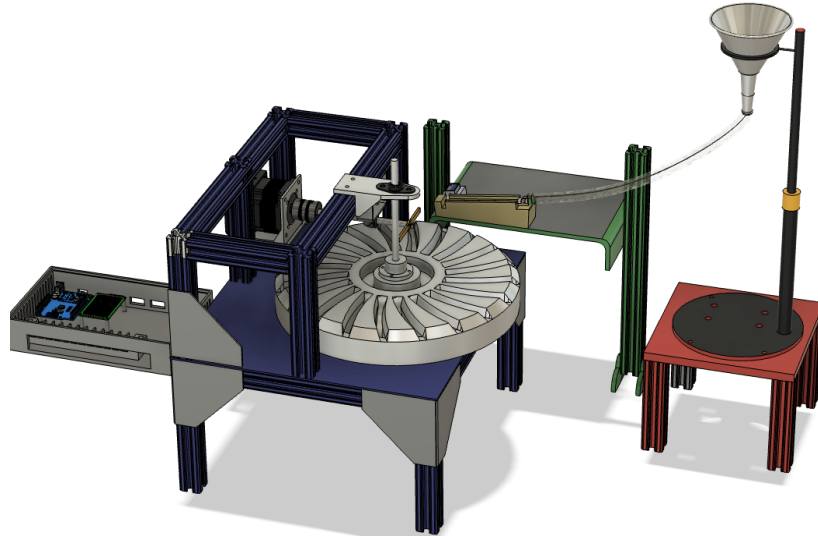
Auto-Loading System Device for Inertial Fusion Energy Power Plant Targetry

Fusion Engineering Institute, UC San Diego

Dr. Javier Garay

General Atomics

Dr. Neil Alexander



J. Ramirez, R. Harun, R. Khalid, T. Prakash and C. Hettinger

MAE 156B- Fundamental Principles of Mechanical Design II

M. Ghazinejad, J.A. Cotrina

8 June 2025

Abstract

Following the 2022 breakthrough in inertial confinement fusion (ICF), there is growing interest in developing scalable systems to support continuous, high-frequency target injection for future fusion power plants. In this capstone project, conducted in collaboration with the Fusion Engineering Institute at UC San Diego and General Atomics, we designed and prototyped an automated system capable of preparing and delivering spherical fusion targets at 0.25 Hz. The system integrates four core components: an input funnel for target batches, a solenoid-actuated gate for controlled single-target dispensing, a rotary fueling disk with evenly spaced grooves, and an ejection arm that conveys targets outward. Each subsystem was developed with modularity, precision, and eventual compatibility with vacuum and cryogenic environments in mind. Design challenges included working with fragile targets ($\sim 30 \mu\text{m}$ wall thickness), staying within a 1 m^3 spatial constraint, and considering future scalability. Testing with surrogate targets showed consistent single-target dispensing without jamming, indicating that the prototype offers a promising starting point for next-generation ICF target delivery systems.

Table of Contents

| | |
|---|-----------|
| Abstract..... | 2 |
| List of Figures..... | 5 |
| List of Tables..... | 7 |
| Chapter 1: Project Background..... | 8 |
| 1.1 Background..... | 8 |
| 1.2 Review of Existing Solutions..... | 9 |
| 1.2.1 Other Types of Target Preparation..... | 9 |
| 1.3 Statement of Requirements..... | 10 |
| 1.4 Deliverables..... | 10 |
| Chapter 2: Description of Final Design Solution..... | 12 |
| 2.1 Cryogenic and Vacuum Compatibility..... | 15 |
| Chapter 3: Design of Key Components..... | 16 |
| 3.1 Target Dispenser and Gate System..... | 16 |
| 3.1.1: Overview..... | 16 |
| 3.1.2 Target Dispenser and Gate System Function Requirements..... | 16 |
| 3.1.3 Funnel Intake System Final Design Choice and Justification..... | 17 |
| 3.1.4 Gate System Design and Justification..... | 17 |
| 3.1.5 Fabrication Details..... | 18 |
| 3.2 Fueling Rotor and Ejection Arm..... | 19 |
| 3.2.1: Overview..... | 19 |
| 3.2.2 Fueling Rotor Function Requirements..... | 19 |
| 3.2.3 Comparison of Designs Considered..... | 19 |
| 3.2.4 Final Design Choice and Justification..... | 21 |
| 3.2.5 Prototype Assembly..... | 23 |
| 3.3 Fueling Stage Actuators..... | 23 |
| 3.3.1 Overview..... | 23 |
| 3.3.2 Functional Requirements..... | 23 |
| 3.3.3 Comparison of Designs Considered..... | 24 |
| 3.3.4 Final Design Choice and Justification..... | 24 |
| 3.4 Control System..... | 24 |
| 3.4.1 Overview..... | 24 |
| 3.4.2 Functional Requirements..... | 24 |
| 3.4.3 Comparison of Control System Interfaces..... | 25 |
| 3.4.4 Final Design Choice and Justification..... | 25 |
| Chapter 4: Prototype Performance..... | 27 |
| 4.1 Theoretical Predictions..... | 27 |

| | |
|---|-----------|
| 4.1.1 System Prototyping..... | 27 |
| 4.1.2 Fueling Stage Analysis..... | 27 |
| 4.2 Test Conditions..... | 28 |
| 4.3 Results..... | 29 |
| 4.4 Comparison to Initial Performance Requirements..... | 30 |
| Chapter 5: Design Recommendations and Conclusions..... | 32 |
| 5.1 Design Recommendations for Future Development..... | 32 |
| 5.2 Mass Production Considerations and Cost Analysis..... | 33 |
| 5.3 Safety Considerations..... | 33 |
| 5.4 Applicable Standards..... | 34 |
| 5.5 Impact on Society..... | 34 |
| 5.6 Professional Responsibility..... | 35 |
| 5.7 Lessons Learned..... | 35 |
| 5.8 Conclusions..... | 36 |
| Acknowledgements..... | 38 |
| References..... | 39 |
| Appendix A: User Manual..... | 40 |
| Appendix B: Fabrication Instructions for Additional Units..... | 43 |
| Appendix C: Technical Drawings..... | 45 |
| Appendix D: Analytical Methods..... | 49 |
| Appendix E: Budget..... | 50 |
| Appendix F: Project Management..... | 56 |
| F.1: Task Distribution..... | 56 |
| F.2: Intermediate Milestones..... | 56 |
| F.3: Risk Reduction Efforts..... | 57 |
| F.4: Lessons Learned..... | 58 |
| F.5: Individual Component Analysis | |
| F.5.1: Ravi Harun - Machining, Manufacturing and Fabrication..... | 58 |
| F.5.2: Tanmay Prakash - Failure Prevention Analysis and IFE Target Simulations..... | 58 |
| F.5.3: Colby Hettinger - Material Selection..... | 58 |
| F.5.4: Rayyan Khalid - CAD Design and Animation of the Rotary system..... | 59 |
| F.5.5: Julian Ramirez - Rotational Actuator Integration..... | 65 |
| Appendix G: Executive Summary..... | 69 |

List of Figures

Figure 1.1: (a) Artist's interpretation of an inertial fusion event via the laser indirect drive scheme. (b) Laser Preamplifiers at NIF

Figure 1.2: Schematic representation of capsule preparation assembly using layering beds and rotary disks

Figure 2.1: Flow chart showing the motion of the target from storage until fueling

Figure 2.2: Drawing of the fueling stage

Figure 2.3: Isometric view of the Autoloader with independent and non-fixed gate and storage system

Figure 2.4: Top view of the Autoloader

Figure 3.1: Intake Funnel System

Figure 3.2: Design of Gate System

Figure 3.3: (a) CAD Top view of Fueling Rotor. (b) CAD of fueling stage assembly, inset: zoomed view of ejection arm

Figure 3.4: (a) Image of Ejection Arm passing through fueling groove. (b) Example of ejection arm twisting found to best remove targets from groove during testing

Figure 3.5: Image of interior of control box demonstrating the master control circuitry and arduino integration

Figure 3.6: Circuit diagram for the master control system

Figure 4.1: Comparison of a mechanically timing belt and pulley system (left) and an electronically synchronized dual-motor system (right)

Figure 4.2: Fueling durations of 240 degrees (left), 180 degrees (center), and 120 degrees (right) of rotary plate rotation

Figure 4.3: Ejection frequency vs. fueling time for different rotor segment angles

Figure C1: Old design of the rotary disk

Figure D1.1: Kinematic diagram of the fueling stage

Figure G.1: CAD of Autoloader Device.

Figure G.2: The Final Autoloader Assembly

List of Tables

Table 3.1: Comparison of Fueling Rotor Articulations

Table 3.2: Comparison of Motors Considered

Table 3.3: Comparison of Control System User Interfaces

Table 4.1: Test results with different rotor speeds

Table 4.2: Prototype Performance Compared to Initial Requirements

Chapter 1: Project Background

1.1 Background

Inertial Fusion Energy (IFE) is a promising approach to nuclear fusion. It uses intense laser light to uniformly compress a spherical fuel target to pressures and temperatures that induce fusion, as shown in Figure 1.1a [1]. This method has recently demonstrated net energy gain at the National Ignition Facility (NIF, Figure 1.1b), and has therefore set precedent as a viable path towards future clean energy [2-4]. However, for IFE to be commercially viable, reactions must occur at high repetition rates, approximately 1-10 Hz, far beyond current single-shot experimental capabilities [1].

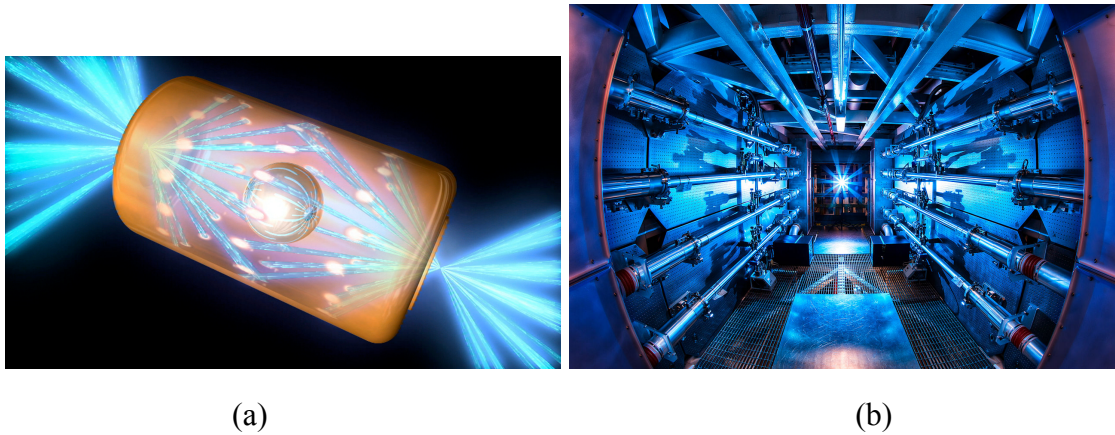


Figure 1.1: (a) Artist's interpretation of an inertial fusion event via the laser indirect drive scheme. (b) Laser Preamplifiers at NIF. Images are public domain courtesy of the United States Department of Energy.

The Fusion Engineering Institute at UC San Diego and General Atomics have begun the Target Injector Nexus for Experimental Development (TINEX) collaboration among several other institutions to improve systems that inject fusion targets into the reactor chambers [5]. A significant priority of this work is developing systems that can facilitate fusion experiments at higher repetition rates. To meet this challenge, Dr. Javier Garay of the Fusion Engineering Institute and Dr. Neil Alexander of General Atomics have sponsored our team to develop a mechanical prototype of an IFE target injector that automates preparation and conveyance of fusion targets.

This system, the Autoloader, is designed to receive batches of empty, 4.5-mm-diameter target shells, individually stage them for fueling and inspection, and transfer them towards a reactor injector at a cycle rate of 0.25 Hz minimum. It is also designed to be readily outfitted with suitable vacuum- and cryogenically- compatible materials expected of real experimental

conditions. The Autoloader ensures precise mechanical handling of the fragile targets with articulations that impart contact forces onto the targets far below their fracture strength. By steadily conveying these targets, the Autoloader demonstrates a solution for future higher repetition-rate fusion experiments, assisting in bringing experimental capabilities to reactor-relevant conditions.

1.2 Review of Existing Solutions

The Autoloader is a unique device to stage fusion targets for preparation and ejection. Numerous target injector concepts have been developed for commercial IFE, particularly among the private start-up sector, however many of these systems are designed for already prepared batches of fusion targets [6-8]. Our sponsor is interested in developing an assembly ahead of the injector to perform fueling on a batch of target shells. Mechanical precision and fragility of these targets makes large-scale target manufacturing a highly technical process [9]. The Autoloader builds off of these efforts by providing a novel bridge between manufacturing and injection into a reactor chamber by mechanizing the fueling and dispensation of these targets toward the injector.

1.2.1 Other Types of Target Preparation

One conceptual IFE target fueling process involves placing targets into cryogenically fluidized layering beds, and transferring them to a rotating loading disk lined with individual target carriages, or “hohlraums,” lining its perimeter. This configuration is illustrated in Figure 1.2. This system outlines a similar operating principle as the Autoloader, which provides a mechanical solution to the “layering beds” concept.

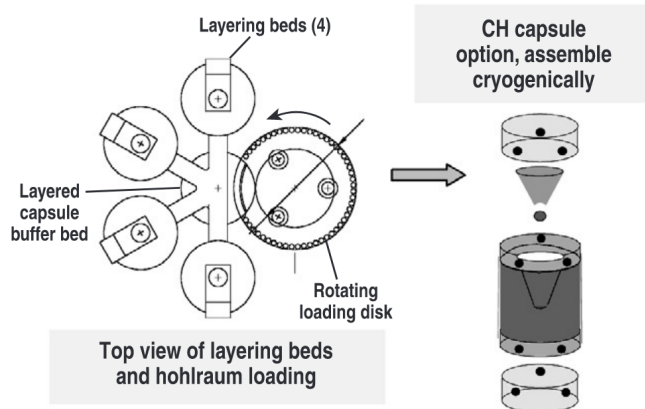


Figure 1.2: Schematic representation of capsule preparation assembly using layering beds and rotary disks [9].

1.3 Statement of Requirements

The following technical and functional requirements were defined for our system through close collaboration with our sponsors and team members:

1. Overall System Requirements

- a. All non-electrical (i.e., motors, circuitry, etc.) components must be compatible with ultra-high-vacuum environments (~ 0.5 mTorr) to prevent outgassing and contamination [10].
- b. The system must be cryogenically compatible down to 20 K, requiring appropriate material selection and geometry to account for thermal contraction and brittle failure risks.
- c. The system must accept a batch of unorganized target shells and autonomously dispense them one at a time at a minimum cycle rate of 0.25 Hz.
- d. System design must allow for modular substitution with vacuum- and cryo-rated components for future reactor integration.

2. Target Handling Requirements

- a. Target shells are extremely fragile (nominal wall thickness ~30 μm); they must be handled delicately, avoiding shear forces or abrupt loading.
- b. Each target must be immersed in a liquid hydrogen fuel bath for a minimum of 10 seconds to ensure proper fuel saturation.
- c. The fueling stage must allow for unobstructed optical access to enable real-time visual inspection of fuel absorption.

1.4 Deliverables

The final deliverables for this project are listed below and reflect the culmination of design, testing, and documentation efforts completed during MAE 156B.

- Fully Functional Prototype:

A working autoloader system consisting of an intake funnel, gated dispenser, rotary fueling rotor, and ejection arm arm, capable of operating at a minimum shot-rate of 0.25 Hz.

- CAD Assembly Model:

3D CAD model of the entire system, including all subsystems, components

- Engineering Drawings:

Detailed fabrication drawings for all custom parts, compliant with ISO 128-1:2020 standards. These include part tolerances, material specifications, and machining details.

- System Documentation:
A complete design report detailing design decisions, analysis, test results, and future recommendations. The report includes sections on safety, professional responsibility, societal impact, and manufacturing guidelines.
- Component Compatibility Guide:
A list of vacuum- and cryogenically-compatible material substitutes for key components such as bearings, motor enclosures, structural elements, and lubricants, to aid future upgrades.
- Bill of Materials (BOM):
An itemized list of all parts used in the prototype, including off-the-shelf components and fabricated parts, with sourcing information and cost estimates.
- Operating and Safety Manual:
A user-facing manual describing safe startup, operation, and maintenance procedures for the prototype, along with troubleshooting steps and usage constraints.
- Analysis and Simulation Appendices:
Supporting documentation for design analysis, including simulations of rotor/ejection arm synchronization, target path kinematics, and stress evaluations.
- Recommendations for Integration and Scaling:
A summary of proposed upgrades for future iterations, including changes in actuation methods, environmental compatibility adaptations, and system expansion for increased throughput.

Chapter 2: Description of Final Design Solution

The final design for the Sabot Autoloader and Recovery System is a fully mechanical, cryogenic- and vacuum-compatible system engineered to automate the precise handling of delicate IFE targets for fusion power applications. The system consists of three main subsystems: the Storage Funnel System, the Target Dispenser, and the Rotary Fueling and Recovery Assembly (see Figure 1.0). Together, these components fulfill the project's primary goals - ensuring safe, repeatable, and efficient handling of fuel capsules with minimal human intervention.

The process begins with the Storage Funnel System, which simulates a large-scale storage setup and ensures a steady feed of IFE targets to the downstream dispenser. It guides targets into a single-file stream suitable for timed dispensing (Step 1).

Next, the Target Dispenser receives the targets from the funnel and releases them at a frequency of 0.25 Hz using a timed solenoid-based actuation system. This ensures synchronization with the fuel staging mechanism (Step 2).

The Rotary Fueling Assembly (Step 3) is the core of the system. It performs multiple functions: injecting targets with fuel, enabling inspection, and handing off targets for injection into the accelerator. Targets are dispensed into precision-machined grooves on a rotating disk, which revolves at a set angular velocity controlled by a stepper motor. This controlled rotation gives sufficient time for each target to be fueled and inspected. The rotation rate is adjustable, allowing for desired operational frequency. Once the fueling and inspection cycle is complete, an ejection arm mechanism synchronized with the disk motion scoops the targets out of their grooves and transfers them for final use. Figure 2.1 illustrates this operational flow from storage to fueling and inspection.

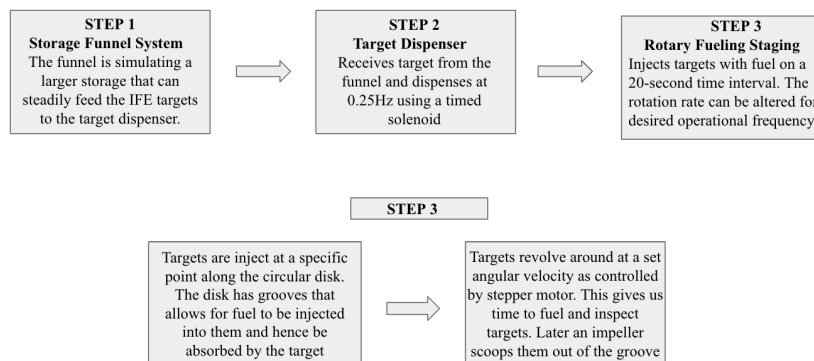


Figure 2.1: Flow chart showing the motion of the target from storage until fueling.

The design of the Rotary Fueling Assembly (also shown in Figure 2.2) includes a 20-slot disk that ensures each target is securely held and properly exposed to the fueling and inspection processes. Spiral groove geometry was implemented to prevent collision during ejection and was validated through simulation and experimental prototyping. As the disk rotates, the dual-arm ejection arm system - geared with a 1:10 ratio to the rotor - synchronously removes the fueled targets at the correct angular positions.

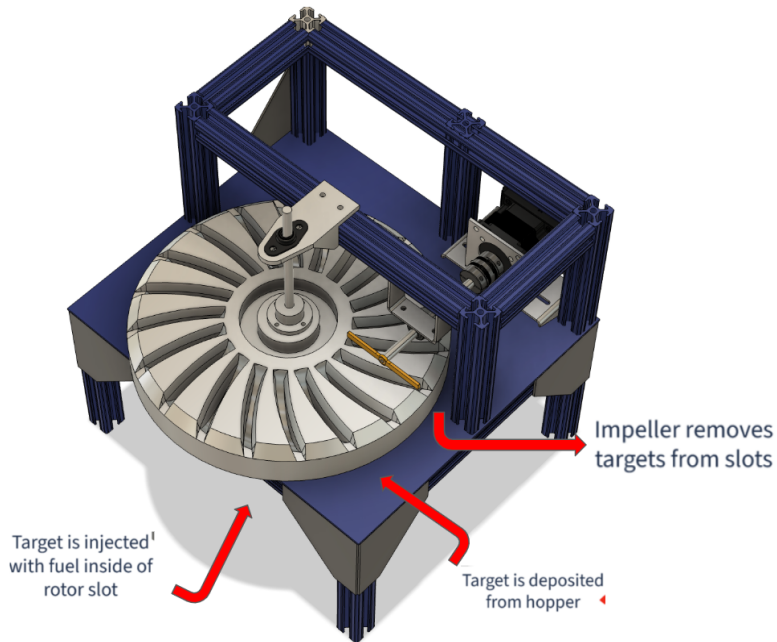


Figure 2.2: Drawing of the fueling stage.

All mechanical components were machined from aluminum for cryogenic compatibility and ease of fabrication. The rotor was produced using tapered end mills on a three-axis CNC system to achieve the required precision. The system was designed with leak-proof slot architecture and minimal interstitial gaps to prevent fuel leakage and maintain vacuum integrity.

In summary, the Sabot Autoloader and Recovery System is a modular, precise, and robust assembly that automates the looped operation essential for IFE reactor functionality. Subsystems were prototyped iteratively and tested for integration, resulting in a mechanically coordinated and operationally validated solution. Further subsystem breakdowns are presented in subsequent chapters.



Figure 2.3: Isometric view of the Autoloader with independent and non-fixed gate and storage system.

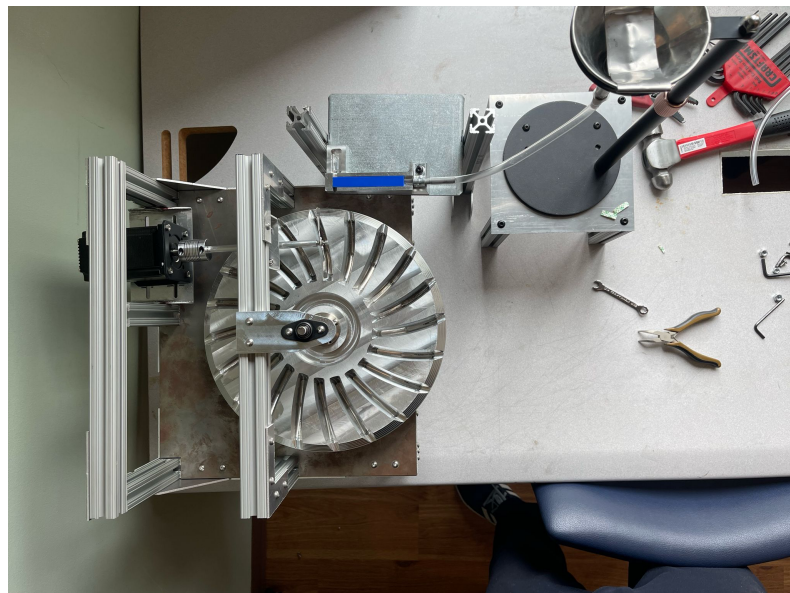


Figure 2.4: Top view of the Autoloader.

2.1 Cryogenic and Vacuum Compatibility

Given the operational context of Inertial Fusion Energy (IFE) environments, where extreme conditions such as cryogenic temperatures and high-vacuum conditions are prevalent, our design aimed to achieve maximum compatibility with these constraints while staying within the economic bounds of a prototyping phase.

To that end, most structural and load-bearing components were machined from 6061 aluminum alloy, a material known for its excellent strength-to-weight ratio, corrosion resistance, and reliable performance in low-temperature and vacuum applications. Its widespread availability and cost-effectiveness made it an optimal choice for iterative development.

However, full-scale deployment of this system in a cryogenic and vacuum environment would necessitate targeted upgrades to several subsystems:

Bearings:

Our current prototype uses self-aligning bearings and ball bearings to support the ejection arm and rotor shafts. These components, typically lubricated with grease, are not suitable for vacuum or cryogenic environments due to outgassing and lubricant failure at low temperatures.

Recommended upgrade: Use dry-lubricated or solid-lubricant bearings such as ceramic hybrid bearings or PTFE-coated stainless steel bearings, which are specifically rated for cryogenic and vacuum operation.

Turntable Support System:

The current rotary disk rests on a standard mechanical turntable, which may not function reliably under low temperatures and pressure.

Recommended upgrade: Replace with a cryogenic-compatible rotary stage, such as those using cross-roller bearings with vacuum-rated stepper motors. These are commonly used in aerospace and semiconductor applications.

Electronic Isolation:

To prevent component degradation or failure due to thermal stress and vacuum exposure, all actuation and control electronics should be physically isolated from the cryogenic chamber.

Recommended approach: Utilize vacuum feedthroughs for signal and power delivery, and enclose electronics in ambient-temperature, shielded compartments. Fiber-optic communication and remote motor controllers can be implemented for improved EMI resistance.

Future iterations should also consider:

- Use of cryogenic-rated stepper motors or piezoelectric actuators.
- Sealing components with metal gaskets instead of elastomeric O-rings to prevent outgassing.
- Designing all moving components to operate without traditional lubricants, instead relying on solid-lubricant coatings or ceramic interfaces.

These proposed modifications ensure that the system can be adapted for high-fidelity testing and eventual deployment in IFE environments, while retaining the modularity and manufacturability established during the prototyping phase.

Chapter 3: Design of Key Components

3.1 Target Dispenser and Gate System

3.1.1: Overview

To enable continuous fueling of inertial fusion targets, the autoloader system must take in a bulk quantity of spherical targets and dispense them individually and reliably into the fueling rotor. This task is accomplished through a two-part subsystem: a funnel-based intake and a solenoid-actuated gate dispenser. Together, these components are responsible for ensuring consistent target flow, avoiding jamming, and delivering single targets at regular intervals.

3.1.2 Target Dispenser and Gate System Function Requirements

The target delivery subsystem must:

- Hold a bulk supply of spherical IFE targets (~3 mm diameter).
- Dispense one target at a time with high reliability and no jamming.
- Prevent damage to fragile targets (thin wall ~30 μm).
- Deliver the target accurately into the rotary disk groove in sync with disk position.

- Be modular and adjustable to match positional requirements of the autoloader.

3.1.3 Funnel Intake System Final Design Choice and Justification

The initial concept called for a vibratory funnel feeder to manage target flow. However, early testing revealed that isolating vibration in a localized region while preventing interference with surrounding components was impractical. Instead, a simpler and more elegant solution was implemented. A V-shaped stopper, fabricated from bent sheet metal, was mounted above the funnel spout to control the flow of incoming targets. This effectively distributes the load and prevents targets from dropping directly into the funnel throat, thereby eliminating jamming without the need for vibration. Targets flow down from the funnel into a 6 mm inner diameter flexible PVC tube, which ensures that only one target can pass through at a time. The other end of the PVC is fitted to a 6 mm aluminum tubing segment, which is bolted to the gate assembly using a custom U-bracket for rigid mounting. This tubing system provided a low-cost, off-the-shelf solution that maintains linear flow control.

The funnel is supported by a height-adjustable stand, and the base was modified using a custom T-slot base plate fabricated in the machine shop to position the funnel at the correct elevation above the fueling stage.



Figure 3.1: Intake Funnel System

3.1.4 Gate System Design and Justification

The gate system is responsible for delivering one target at a time into the fueling disk grooves, aligned with the rotary cycle. Originally, a two-gate configuration was considered to prevent

backflow and accidental injection of multiple targets. It would work by having one target between the two gates and dispensed at regular time intervals by opening only the end gate. However, during conceptual discussions, a major flaw became apparent: in a two-gate configuration, when the first gate retracts to release a target, additional targets from the bulk queue tend to flow into the vacated space. As the gate attempts to close again, one of these targets can obstruct the path and be forcibly pushed or crushed by the closing motion.

To solve this, the team opted for a single-solenoid configuration, reversing the traditional logic of a "gate opening" and instead using a linear solenoid to push the target forward, ejecting it into the disk in the direction of what would conventionally be considered "closing" the gate. This not only simplifies control logic but also eliminates the risk of crushing fragile targets, which are highly sensitive due to their $\sim 30 \mu\text{m}$ wall thickness.

The gate angle was also a crucial parameter. Through a series of bench-top experiments with mock targets and variable inclination angles, the team identified 7.5 degrees as the optimal incline for ensuring smooth, gravity-assisted flow without allowing uncontrolled acceleration. This angle was then locked into the final design.

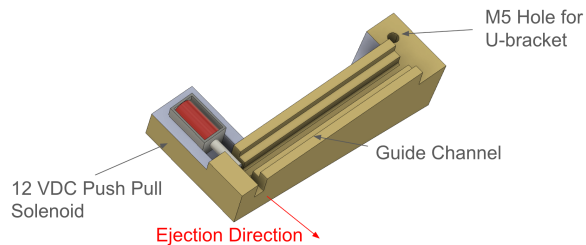


Figure 3.2: Design of Gate System

3.1.5 Fabrication Details

The gate assembly was machined from a single block of Aluminum 6061 using a HAAS Mini Mill. The stock was angled at precisely 7.5 degrees on the setup table, and the middle slot for the solenoid and target channel was cut using an end mill for smooth, dimensionally consistent walls. Mounting holes were tapped for attaching the U-bracket and aluminum tubing.

The overall assembly is compact, mechanically robust, and integrates seamlessly into the rest of the autoloader system. To ensure alignment between the gate output and the fueling rotor grooves, the gate system is mounted on a height-adjustable support platform. This platform uses T-slot vertical legs that allow the gate assembly to be raised or lowered with fine control, improving system modularity and adaptability to future component changes. It has performed reliably under testing, dispensing one target per solenoid actuation with high repeatability and zero observed jamming or damage to the target surrogates.

3.2 Fueling Rotor and Ejection Arm

3.2.1: Overview

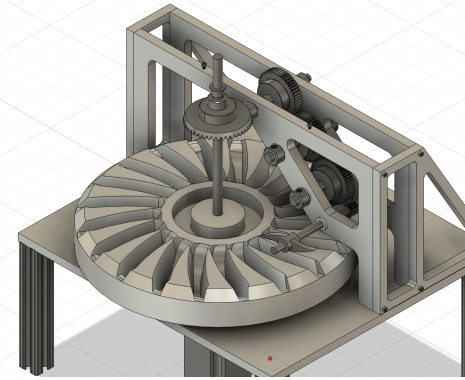
The function of the fueling rotor and ejection arm is to allow for synchronized fuel injection, saturation time, inspection, and conveyance of individual targets with minimal impact forces or momentum impulses on them. Targets are sent into a fueling rotor groove from the gate system. As the disk rotates, a target slot can pass by a fuel injector to be doped, and have time for saturation during its travel towards the ejection arm. The ejection arm rotates at a related rate to the fueling rotor and scoops each fueled target out of the groove towards the next stage. Appendix D1 describes how the geometry of these grooves were determined to facilitate smooth ejection arm passage.

3.2.2 Fueling Rotor Function Requirements

- Made of vacuum- and cryogenically-compatible materials
- Does not load or shear the targets
- Allows for 10 seconds fuel saturation time
- Allows for side-on imaging of targets after fueling for absorption inspection
- Ejects targets at minimum 0.25 Hz cycle rate

3.2.3 Comparison of Designs Considered

Table 3.1: Comparison of Fueling Rotor Articulations

| Design Ideas | Pros & Cons |
|--|---|
|  <p>Gear Train Assembly</p> | <p>Pros:</p> <ul style="list-style-type: none"> • Greatest reliability and timing precision between rotor and ejection arm <p>Cons:</p> <ul style="list-style-type: none"> • High mechanical complexity • Precision alignment required • Must outsource manufacturing to achieve adequate precision |
|  <p>Dual-Motor Assembly</p> | <p>Pros:</p> <ul style="list-style-type: none"> • Less machining required • Easy to adjust components for proper alignment and timing • Fewer parts <p>Cons:</p> <ul style="list-style-type: none"> • Motor synchronization depends on controller • Less timing precision than gear train |

3.2.4 Final Design Choice and Justification

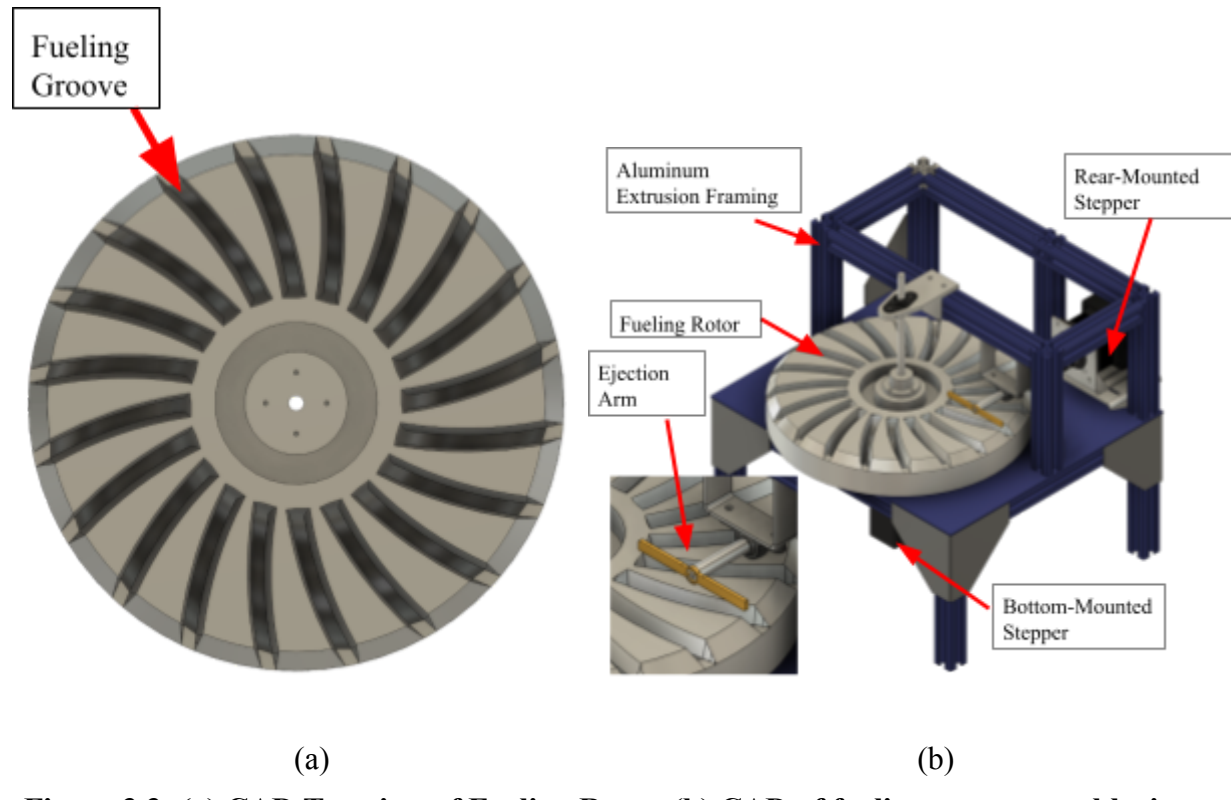


Figure 3.3: (a) CAD Top view of Fueling Rotor. (b) CAD of fueling stage assembly, inset: zoomed view of ejection arm.

The final design of the fueling stage, as depicted in Figure 3.3, utilizes the dual-motor design, as it provides the most adjustability in alignment and timing between the rotor and ejection arm. The fueling rotor and ejection arm rotate continuously; the rotor has 20 grooves, and the ejection arm has two arms, therefore spin relative to each other via a 1-to-10 angular speed ratio. As the fueling disk and ejection arm rotate simultaneously, each groove's slot traces an arc that allows the ejection arm to pass through without hitting the walls of the groove. This arc constitutes a section of a spiral defined by the rotor and ejection arm geometry. The derivation of the equation used for the groove profile geometry to achieve this may be found in Appendix D1.

The 280-mm-diameter (~11 in) rotary fueling disk was CNC machined from 12-in-diameter by 2-in-thick Aluminum 6061 stock on a Haas VF2 milling machine in the UCSD MAE Machine Shop. It rests on a ball-bearing turntable, and sits on a 310 mm by 350 mm (12.2 in by 13.78 in) frame constructed of laser cut steel sheet metal and aluminum extrusions. A stepper motor mounted on the bottom side of the frame actuates the rotor from below through an attached shaft.

The shaft is constrained via the vertical ball bearing on the top of the frame as seen in Figure 3.3b.

The ejection arm is 80 mm (~3.15) in diameter, and was fabricated from aluminum sheet metal via laser cutting. Testing demonstrated that the ejection arm performed best when each arm was slightly twisted by hand at each end. The ejection arm is screwed in place to a shaft, and directly actuated via a stepper motor on the rear of the frame. Figure 3.4 shows the ejection arm passing through a fueling rotor groove as they rotate simultaneously, and Figure 3.4b shows an example of the ejection arm twisting that resulted in more efficient conveyance of targets out of the grooves.

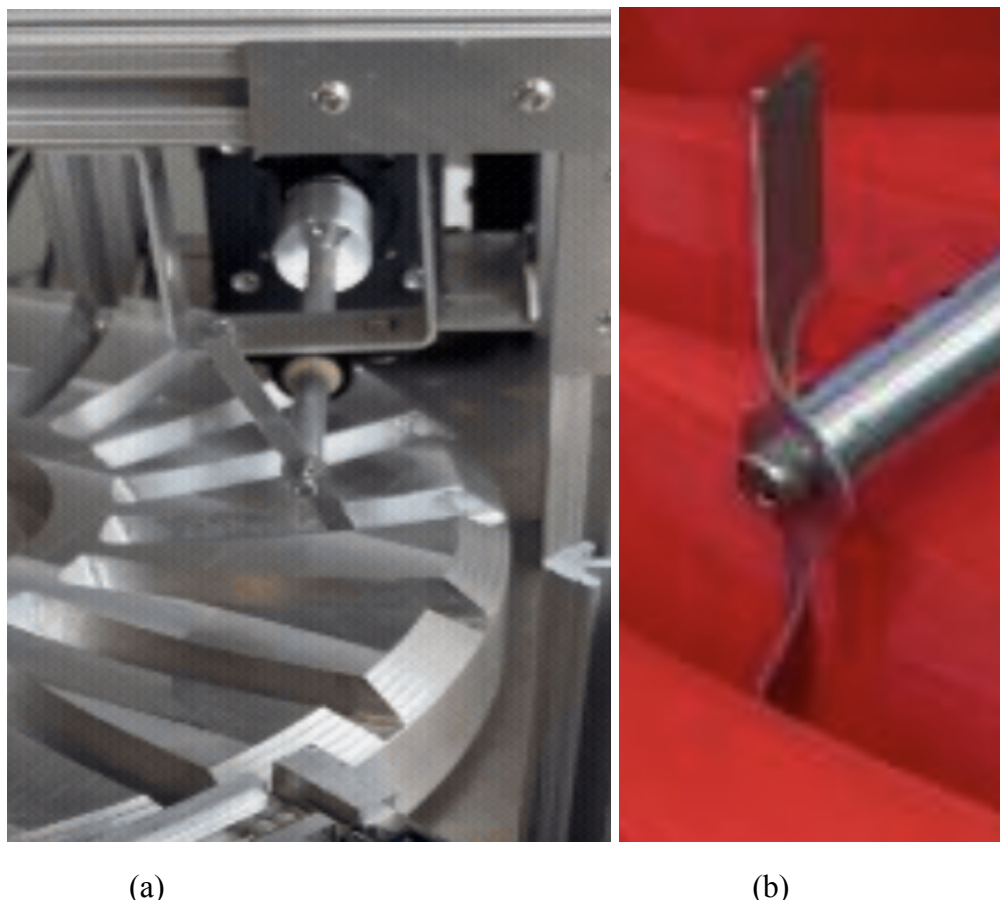


Figure 3.4: (a) Image of Ejection Arm passing through fueling groove. (b) Example of ejection arm twisting found to best remove targets from groove during testing.

3.2.5 Prototype Assembly

The final prototype was assembled on a flat laser-cut steel base plate. The supporting structure was built using T-slotted aluminum framing, which provided modularity and allowed precise mounting of rotary shafts and subassemblies. Custom shaft brackets were waterjet-cut from Aluminum 6061 to constrain vertical alignment and maintain clearance tolerances.

The rotary fueling disk was CNC machined from Aluminum 6061 on a Haas VF2 milling machine and features 20 spiral grooves that match the theoretical trajectory defined in Chapter 3.4. During early prototyping, this disk was substituted with a 3D printed version to allow early testing while waiting on the final aluminum part. The ejection arm arm was fabricated from a flat aluminum sheet via laser cutting, then bent to form a dual-arm structure. A flat region was added at the center to enable shaft attachment via a tapped set screw interface.

A NEMA 17 stepper motor was mounted beneath the base plate to drive the rotor. For the single-motor configuration, a direct mechanical coupling was used; for the dual-motor setup, a second stepper was attached to a shaft-mounted ejection arm bracket using a slotted aluminum crossbeam.

3.3 Fueling Stage Actuators

3.3.1 Overview

The fueling stage is actuated by a dual stepper motor setup. They were selected due to the angular precision required for the simultaneous motion between the fueling rotor and ejection arm. LEESN IG57E Series micro-stepper motors were selected for both the actuation of the fueling rotor and the ejection arm. They are controlled via a master arduino control script used across the entire Autoloader system.

3.3.2 Functional Requirements

- Precisely synchronize the motions of the fueling rotor and ejection arm
- Provide enough torque to quickly bring system to a steady state constant angular speed
- Be easily integrated into control system and compatible with Arduino control

3.3.3 Comparison of Designs Considered

Table 3.2: Comparison of Motors Considered

| Model | Holding Torque | Interface |
|-----------------------------------|----------------|---|
| Anaheim Electronics 34MDSI112S | 4.5 Nm | Integrated controller via RS-485 protocol |
| LEESN IG57E | 1.2 Nm | Integrated controller with serial comm. Or micro-USB |

3.3.4 Final Design Choice and Justification

The LEESN IG57E was ultimately selected as it provided adequate torque while being the most readily compatible with an arduino-based controller. Both motors were easily joined into the system, as they both had integrated drivers. However, unlike the 34MDSI112S series, which uses a proprietary control program, the IG57E can directly communicate via serial commands at the terminal bus, which could then be controlled using Arduino.

3.4 Control System

3.4.1 Overview

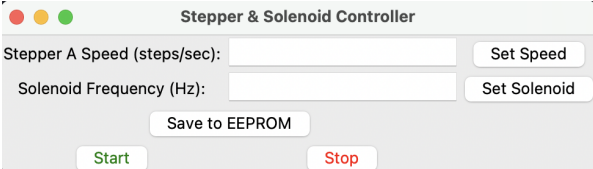
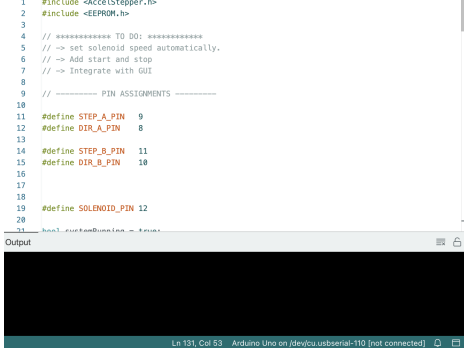
The entire Autoloader assembly is controlled by a master Arduino controller unit that allows users to define the stepper motors speeds and the solenoid thrust frequency. The arduino platform was chosen due to its simplicity, ubiquity, and rapid-prototyping capabilities. The controller is contained within a centralized control box unit that can be placed adjacent to the system, and outside of vacuum to prevent electronics being damaged by reactor conditions.

3.4.2 Functional Requirements

- Capable of driving both motors simultaneously
- Capable of driving the solenoid gate
- Synchronicity between all actuators
- Easily controllable by a new user

3.4.3 Comparison of Control System Interfaces

Table 3.3: Comparison of Control System User Interfaces

| Interface | Pros & Cons |
|--|--|
|  GUI-Based User Interface | <p>Pros:</p> <ul style="list-style-type: none"> • Accessible by users unfamiliar with Arduino IDE • Simple operating Principle <p>Cons:</p> <ul style="list-style-type: none"> • More work to modify • Cannot readily see what commands are doing directly in the script |
|  Arduino TUI-Based Interface | <p>Pros:</p> <ul style="list-style-type: none"> • Rapid scripting, scales to greater number of components or control logic • WYSIWYG: Exact control logic is immediately visible by the user, and control is highly customizable. <p>Cons:</p> <ul style="list-style-type: none"> • Learning-curve for users unfamiliar with Arduino scripting • Not as easy to input commands |

3.4.4 Final Design Choice and Justification

Ultimately a Arduino TUI-Based controller was chosen as the user interface, since it was the most customizable for later system additions. The control box itself houses the arduino and necessary circuitry to control both motors and solenoid simultaneously, as seen in Figure 3.5. Figure 3.6 shows the wiring diagram used to control all actuators. A 12VDC supply is connected to the solenoid, while a 24VDC supply powers both the stepper motors in parallel. The Arduino is powered by another 12VDC barrel-jack wall adapter. Commands are sent through the Arduino IDE serial monitor via USB, and are written as “commandlets” detailed in a switch case. To control the stepper motors a user sends a command of the form “AX” where X is the speed in steps per second on the motor. To control the solenoid, a user writes “SY” where Y is the push frequency in Hz. Sending “W” to the terminal writes the current settings to the Arduino’s EEPROM if desired for future use.

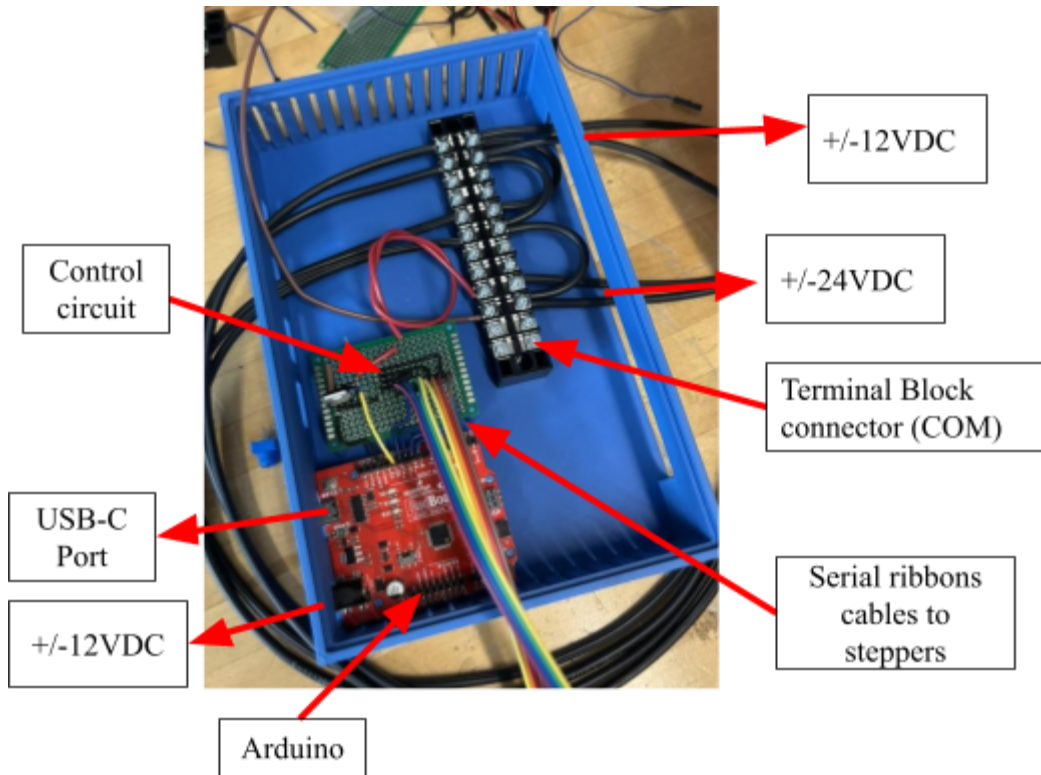


Figure 3.5: Image of interior of control box demonstrating the master control circuitry and arduino integration.

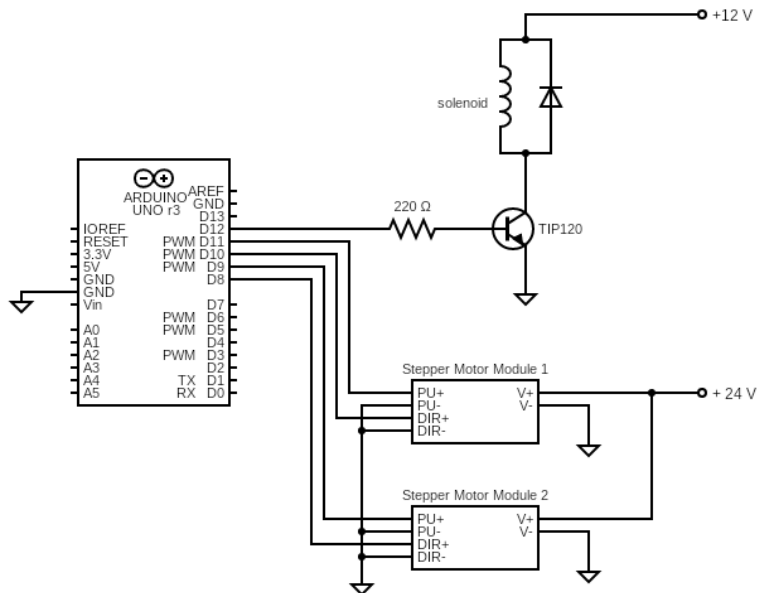


Figure 3.6: Circuit diagram for the master control system.

Chapter 4: Prototype Performance

4.1 Theoretical Predictions

4.1.1 System Prototyping

Two synchronization approaches were prototyped: (1) a mechanically linked timing belt and pulley system, and (2) an electronically coordinated dual-motor system.

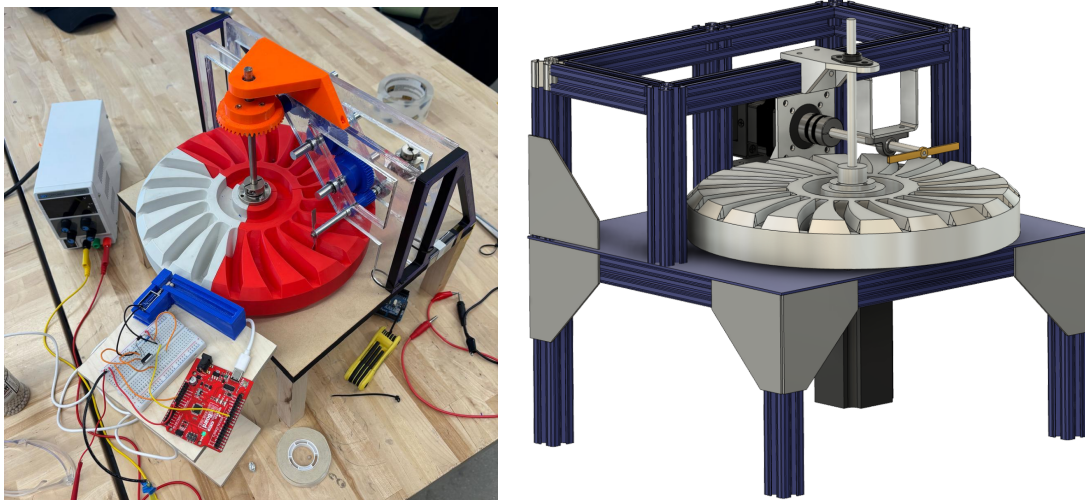


Figure 4.1: Comparison of a mechanically timing belt and pulley system (left) and an electronically synchronized dual-motor system (right).

4.1.2 Fueling Stage Analysis

To optimize the fueling stage, we conducted tests using various segment sizes of the rotary plate. Larger fueling segments provided greater flexibility in meeting the current design constraints. These segment sizes were plotted on a graph (Fig. 4.3), where points in the first quartile fell within the boundaries specified by our sponsor. We selected test points that were well within these limits, aiming for a practical “sweet spot” that balanced performance and design feasibility.

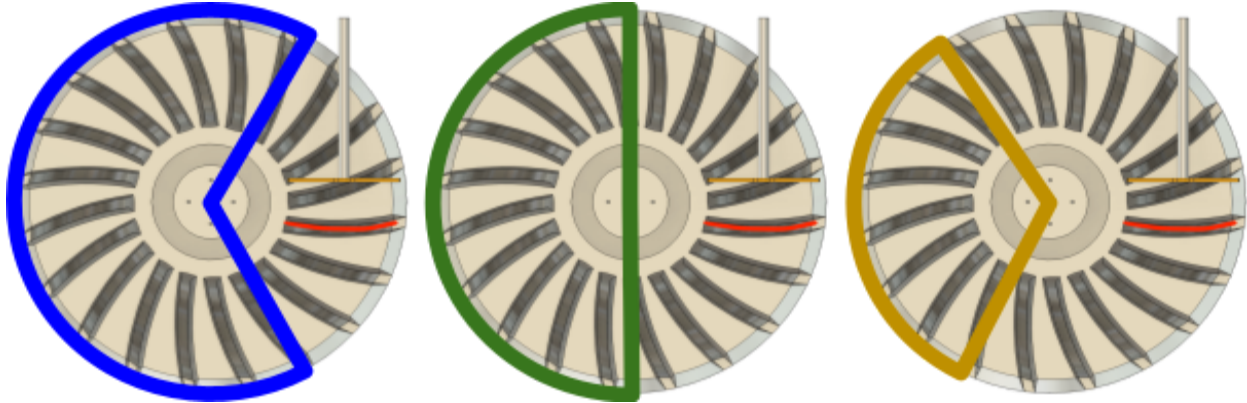


Figure 4.2: Fueling durations of 240 degrees (left), 180 degrees (center), and 120 degrees (right) of rotary plate rotation.

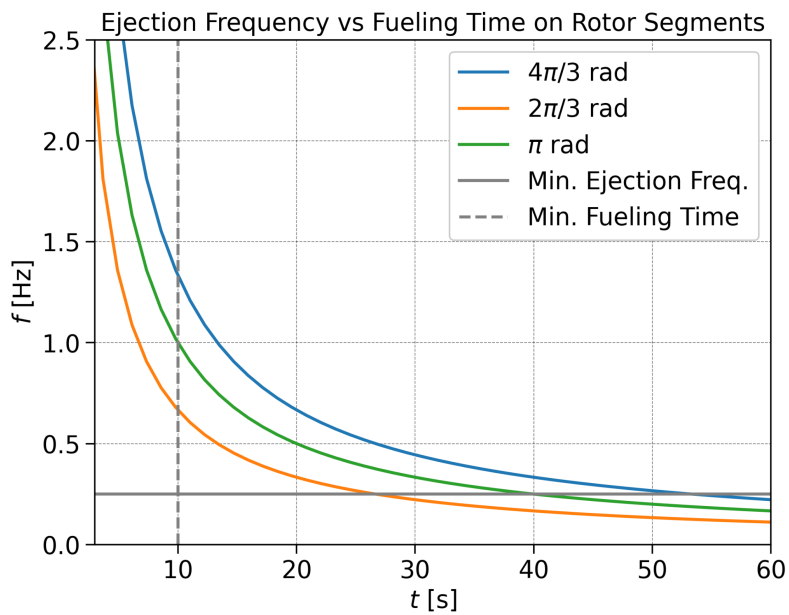


Figure 4.3: Ejection frequency vs. fueling time for different rotor segment angles.

4.2 Test Conditions

Prototype testing was carried out following the completion of the manufacturing phase. A test of ejection success rate was performed. Over three trials at each test point speed, a sample of 20 targets was placed in each groove of the fueling rotor, and the number of targets that were successfully ejected were recorded.

4.3 Results

Testing of the prototype focused on validating functionality across the first part of Phase 1 – target intake and delivery into the rotary fueling disk – and the operation of the rotor-ejection arm synchronization system. A partial mockup of Phase 2 was also developed to explore downstream target transfer.

Phase 1 – Target Loading and Rotary Stage

Table 4.1: Test results with different rotor speeds

| Rotor Speed (rad/s) | Ejection Success Rate (Avg. of three trials) |
|---------------------|---|
| 0.523 | 90% |
| 0.418 | 75% |
| 0.349 | 65% |

Table 4.1 summarizes the ejection success rate data from the ejection test. The gradual decrease in success rate is assumed to be caused largely by systematic error, as calibration inconsistencies between trials made the ejection arm less efficient. Additionally, during testing the ejection arm was bent slightly, which may have contributed to these results.

A vibratory funnel and tubing system was implemented to deliver targets from a bulk container into the rotary fueling disk. Early jamming issues were addressed by installing a mechanical stopper inside the funnel that restricts target flow into the spout, eliminating the need for the previously planned vibratory motor.

The funnel was mounted onto a height-adjustable hardened steel stand and connected to the gate system via aluminum tubing and flexible PVC pipe, which fed directly into a solenoid-actuated gate. This gate was controlled using an Arduino and successfully delivered one target at a time into each groove of the rotating disk.

Initial performance testing focused on validating the mechanical synchronization between the ejection arm arm and the rotary fueling disk, and ensuring the system could dispense targets reliably under continuous operation. Testing was conducted with the 3D printed rotor, aluminum ejection arm, and the two-motor configuration.

Phase 2 – Transfer and Ejection (Preliminary Development)

A separate system mockup was created to test the feasibility of target transfer from the fueling disk to a sabot cartridge using another gate mechanism. When the ejection arm ejects the target, it enters a solenoid-controlled gate that directs it into a sabot mounted on a sliding carriage within a magazine channel. A second solenoid is used to advance the sabot to the ejection bay.

Due to time and resource constraints, Phase 2 components were constructed using 3D-printed housings and laser-cut structures. While not tested under full conditions yet, the gate mechanics and carriage motion are functional, and initial tests show promise for extending the autoloader system beyond fueling.

The system successfully operated at the target shot rate of 0.25 Hz, with no observed mechanical collisions between the ejection arm and groove walls. The spiral groove geometry, derived from theoretical predictions, guided the ejection arm precisely during each pass-through. Across multiple cycles, the ejection arm consistently aligned with the grooves, and targets were transported smoothly without jamming or tipping.

The aluminum ejection arm proved mechanically stable and structurally robust during motion. While target surrogates occasionally shifted slightly within grooves during rotation, all remained retained through the ejection arm engagement phase. Visual inspection confirmed consistent clearance between moving parts, with no noticeable deformation or mechanical wear over repeated use.

Some limitations during testing included:

- Manual timing of solenoid actuation and motor startup, resulting in variability between test runs.
- Occasional slip in target orientation due to inconsistencies in the mock target dimensions and surface finish.
- The pulley synchronization system remains untested as final assembly is still pending.

Despite these constraints, the core mechanical design demonstrated functional viability, with stable operation under expected conditions.

4.4 Comparison to Initial Performance Requirements

The empirical results were benchmarked against the original performance requirements outlined during the design phase. The prototype met expectations in all critical metrics, including synchronization precision, scalability, and mechanical reliability.

The successful validation of theoretical predictions, particularly the performance of the ejection arm through the spiral groove, confirms the feasibility of the Archimedean spiral-based transport mechanism for IFE target fueling. Minor refinements in the control algorithm and groove machining tolerances were identified as potential areas for further optimization. Overall, the prototype demonstrates readiness for further development and higher-frequency scalability in future design phases.

Table 4.2: Prototype Performance Compared to Initial Requirements

| Performance Requirement | Target Specification | Achieved Outcome | Met? |
|--|---|---|------|
| Shot rate | $\geq 0.25 \text{ Hz}$ | $> 0.25 \text{ Hz}$ | Yes |
| Rotor-ejection arm synchronization | Continuous, no collisions | Stable alignment over multiple cycles | Yes |
| Smooth target dispensing | No jamming or target loss | Targets dispensed without mechanical error | Yes |
| Structural durability of ejection arm | No deformation under operation | Aluminum ejection arm retained shape and strength | Yes |
| Groove-ejection arm clearance | Min. 1 mm clearance | Approx. 1.5 mm observed | Yes |
| Cryogenic and vacuum compatibility (design-based only) | Materials upgradable | Compatible materials identified | Yes |
| Pulley-driven operation | Smooth belt-based synchronization | Awaiting full assembly | Yes |
| Target input from bulk funnel | Reliable intake into disk | Stopper prevented jamming; funnel worked well | Yes |
| Gate actuation | Single target release per trigger | Solenoid gates released reliably | Yes |
| Downstream target transfer (Phase 2) | Direct transfer to sabot + ejection bay | Mechanically prototyped, testing in progress | Yes |

Overall, the prototype meets all essential performance goals for mechanical synchronization and operation at baseline shot rate. Once the pulley system is fully assembled and tested, further validation will confirm whether it can offer the expected reduction in complexity and increase in scalability.

Chapter 5: Design Recommendations and Conclusions

As the field of inertial fusion energy (IFE) advances toward becoming a viable source of clean energy, the ability to develop robust, efficient, and scalable target handling systems becomes paramount. This prototype has demonstrated the feasibility of automating the preparation and delivery of IFE targets at a baseline rate of 0.25 Hz. However, transitioning from this prototype to a mass-producible version suitable for actual power plant conditions requires several important design refinements and considerations.

5.1 Design Recommendations for Future Development

First, remaining non-rated components should be replaced with cryogenic- and vacuum-compatible alternatives. This includes replacing the PVC tubing - which may become brittle or outgas under extreme conditions - with metal or PTFE tubing. Additionally, the self-aligning bearing used in the ejection arm shaft should be replaced with a dry-lubricated or solid-state bearing, as conventional grease-lubricated bearings are unsuitable for vacuum environments and can fail at low temperatures. All electrical wiring, adhesives, and seals should also be reviewed for material compatibility with ultra-high vacuum and cryogenic use.

Given that standard motors are not suitable for vacuum or cryogenic environments, future systems should position both the rotor and ejection arm motors outside the chamber, transmitting torque via shaft extensions with vacuum-rated rotary feedthroughs. This approach enables the use of conventional motors while maintaining environmental isolation. Vacuum and cryogenic compatible motors can also be used which can be operated inside without the need to put them out of the system but they will come at a higher cost.

While the current system uses two independently controlled motors, future designs may consider replacing this with a timing belt or gear-coupled solution to maintain a fixed 10:1 ratio between the ejection arm and rotor. This would reduce control complexity and ensure mechanical synchronization, minimizing the risk of misalignment.

Alternatively, if independent motors continue to be used, it is essential to integrate a rotary encoder for the ejection arm. This would allow the system to initialize the ejection arm in the correct phase position, avoiding accidental interference with the fueling rotor grooves. Without proper indexing, the ejection arm risks colliding with the rotary disk.

Additionally, to improve delivery accuracy, the system should implement a feedback control loop between the solenoid gate and rotor position. A simple optical sensor or encoder would allow the solenoid to trigger exactly when a groove lines up, improving target placement and minimizing misfires..

Other design improvements include:

- Oversizing parts during fabrication to account for thermal contraction at cryogenic temperatures.
- Replacing current bearings and bushings with dry-lubricated or solid-state alternatives compatible with vacuum use, as conventional lubricants are ineffective and can outgas.
- Designing the structure with modularity in mind, allowing for easy component replacement or scaling to higher throughput systems (1–10 Hz). This would enable the system to meet varying shot-rate demands in experimental and commercial applications.

5.2 Mass Production Considerations and Cost Analysis

From a manufacturing perspective, we estimate that the cost of each unit would fall in the range of \$2,500 to \$3,000 USD per unit. This estimate accounts for CNC-machined aluminum components, modular framing, actuator systems, and basic control electronics.

The most expensive component is the fueling rotor, quoted at around \$700 if manufactured globally and \$1138 if manufactured in the USA for low-volume machining and standard shipping by Protolabs Network based on our CAD with a medium ISO 2768 general tolerance, with the raw aluminum stock alone costing approximately \$312. The solenoid-based gate system, including hardware, mounts, and wiring, is estimated at \$500, while T-slot profiles and fasteners for the full structure contribute another \$200–250 per unit.

Additional costs include stepper motors (\$221 each), rotary feedthroughs and shaft extenders for vacuum compatibility (\$150 combined), and general wiring, connectors, power supply, and control boards, estimated at \$100–150. Labor and basic assembly overhead account for an additional \$200–300 per unit.

5.3 Safety Considerations

Proper PPE should be assumed when handling the Autoloader System due its metal construction, integrated electrical components, and geometry. Much of the framing has sharp metal edges, like at the aluminum extrusion corners or exposed shafts. Certain components, particularly the fueling rotor, are quite heavy and can easily slip from grasp. We recommend transporting and manually arranging the device with appropriate heavy duty gloves.

Though we have taken as many precautions as possible to hide all exposed wiring, components like the solenoid draw high (~2A) current, and relatively high voltage (12V). It is therefore crucial to power off all electronics before interacting with the circuitry.

As the system evolves, we recommend full enclosures for all moving parts, robust shielding for electrical components, and emergency stops. Working with cryogenic fuels like liquid hydrogen introduces more risks like pressure build-up or thermal shock so future versions should include thermal insulation, venting, and materials rated for low-temperature use. We also recommend the use of sensors for safety. For instance, jam detection or motor overheating alerts could stop the system before damage occurs. Plus, adding basic fault logic in the control software could help avoid unsafe conditions during runtime.

5.4 Applicable Standards

The design and potential deployment of the system must align with key engineering standards to ensure safety, compatibility, and long-term reliability in advanced research and commercial fusion environments. Several specific standards are particularly relevant.

ASME B31.3 governs process piping systems and is critical when interfacing with cryogenic fluids such as liquid hydrogen. This standard ensures proper material selection, welding procedures, and leak testing for high-integrity fluid systems.

ASTM E595 outlines acceptable limits for material outgassing in vacuum environments. Given the ultra-high vacuum (UHV) requirements of inertial fusion systems, components must be evaluated for volatile content to prevent contamination of sensitive equipment.

ISO 14644-1 defines classes of air cleanliness in cleanroom environments. If the system is to be used near sensitive optics or fusion reactors with particulate control requirements, it must comply with relevant cleanroom compatibility standards.

IEEE 1227-1990 provides guidelines for robotic and automated systems operating in hazardous environments. This standard informs the design of motion systems – such as our ejection arm and actuator modules – especially if they are deployed in cryogenic, vacuum, or radioactive conditions.

Adhering to these standards will help ensure that the system can be integrated into both laboratory-scale testing environments and eventual commercial inertial fusion facilities, while maintaining safety and functional reliability.

5.5 Impact on Society

A large driver of global warming is human energy consumption via combustion of fossil fuels and natural gases [11]. Achieving fusion power through IFE would produce abundant energy

with non-harmful byproducts, which has the potential to drastically change the way we generate energy and combat climate change.

The goal of this project was to develop a system that could mechanically stage and prepare fusion targets at a higher cycle rate than current fusion experiments. Target delivery at commercially-viable shot-rates is a key bottleneck in IFE research. Therefore, the Autoloader has the potential to help bring IFE research closer to reactor-relevant shot-rate conditions.

5.6 Professional Responsibility

The Autoloader requires very involved calibration and monitoring, therefore it is crucial for users to understand how to operate the system effectively. To this end, a user's manual is included in this report that outlines how to properly run the system from the first time onwards.

We attest that all findings were recorded in a truthful manner, and we have ensured that we properly documented any potential safety hazards associated with the Autoloader.

We would also like to clarify our intentions with this project. We have sought to advance inertial fusion energy research towards developing clean, carbon-free energy solutions, and potentially nuclear non-proliferation, but not in the pursuit of weapons development. It is our ethical responsibility as engineers to create this device with the intention of helping, rather than harming, humanity.

5.7 Lessons Learned

Throughout the course of this project, we encountered many challenges in defining the project and aligning our capabilities with a feasible end goal. Due to the open-concept nature of the project, we spent prototyping for the entirety of our Winter quarter (MAE 156A) of the project (5 Weeks) and the first half of Spring quarter (about 4-5 weeks of MAE 156B). Our initial prototype for our fueling stage (see appendix Figure C1) involved pins and ramps, which we had spent weeks researching and preparing for our risk reduction presentation. This process was helpful to understand limitations of cryogenic fuelling, an information in which we ultimately used to pivot to another design at the start of MAE 156B (our current one). The lesson learned here is that even a relatively simple conceptual idea—filling and passing spheres (representative of IFE targets)—becomes deeply nuanced when constrained by precision, delicacy, and environmental requirements. Team coordination, iterative prototyping, and a willingness to confront failure were vital lessons we will carry into our future careers.

We also learned to balance innovative design with manufacturability and to test and revise ideas quickly. A significant portion of our prototyping process was dealing with the complexity of rotary systems, which taught us the importance of gearing, alignment, and tolerance control. Through repeated testing and refinement using 3D printed parts, we were able to understand the significance of small alignments to our system's operation but weren't able to start on actuation more rigorously. Specifically, interfacing between mechanical and electrical systems revealed the

practical difficulties of synchronization, timing, and actuation, which emphasizes the necessity of early system integration during the design phase.

Lastly, we encountered a manufacturing delay nearing the end of our project due to a shortage of the synthetic grease oil needed for the Haas VF2SS spindle in the machine shop. This oil was needed to complete the rotary disk, a critical component of our project, and its shortage halted progress for about 4 days in Week 8 of Spring quarter due to our efforts to locate a replacement locally and/or order a verified oil online. This delay resulted in reduced time for testing our system with real machined parts (instead of 3D printed parts). The lesson learned here is that we should have manufactured our machined part earlier in the quarter, preferably Week 5 or 6, in order to account for fabrication bottlenecks similar to the above and allocate more time for testing.

5.8 Conclusions

This project aimed to develop an automated target loading system for inertial fusion energy (IFE) applications. The task at hand was to design a system where IFE targets could be loaded onto a system where each individual IFE target would be fuelled, inspected and loaded into a sabot carriage and shot out onto a linear inductor where a high powered laser would interact with the target and start the inertial fusion process. Moreover, our process would need to happen within high vacuum and cryogenic conditions. Due to the large scope of our project, we defined the project to be solely the loading, fuelling and offloading part of the scope. Alongside that, the cryogenic and high vacuum environment conditions were kept in mind while designing for our system and we thought of alternative materials that would be easily replaceable in the actual system. This allowed us to focus on a specific area of the project and optimize our efforts.

Our final system demonstrated a successful handling of IFE targets and a fully adjustable system for General Atomics and UC San Diego engineers to run the system at different ejection rates. More specifically, engineers operating our system would be able to pour bulk IFE targets into a funnel leading to a gate system, which would then load targets into the rotary disk at desired ejection rates. The rotary disk has 20 grooves to accommodate loading and off-loading of targets from the gate system and by an ejection arm, respectively. Additionally, these grooves are designed to securely house these IFE targets and minimize fuel loss during fueling. This is achieved through grooves that are precisely machined with a geometry that eliminates gaps or sharp edges where fuel could seep out, ensuring an optimized clean and efficient target fueling. Then, targets within these grooves would be dispensed at a rate of 0.25 Hz with an ejection arm that follows the curvature of our rotary disk, achieving our main functional requirement.

For future development, all non-rated materials, such as PVC tubing, grease lubricated bearings and wirings, should be replaced with high vacuum and cryogenically compatible materials. Moreover, our stepper motors should either be relocated to outside the chamber with connections to inside the chamber or replaced with a motor compatible with those conditions. Another crucial part of our system is phase alignment between our solenoid powered gate system and rotary disk

and dual ejection arm with our rotary disk. To prevent misalignment, the dual ejection arm should be installed with a rotary encoder, and solenoid triggers should be tied to the rotary disk's rotation via a feedback loop using optical sensors. Additionally, synchronization between the rotary disk and ejection arm can be improved using timing belts or gear coupling. Lastly, improvements should include oversizing parts to account for thermal contraction due to cryogenic conditions. This ensures our design is modular enough for scalability and components meet sponsor requirements of high vacuum and cryogenic standards.

Acknowledgements

Our team would like to thank the following individuals for their contributions to this project:

Instructors: Dr. Maziar Ghazinejad

Jackelin Amorin Cotrina

Sponsors: Dr. Javier Garay

Dr. Neil Alexander

Engineering Staff: Stephen Mercsak

Tom Chalfant

Hussein Ashour

David Lesser

Edward Poque

Thank you for your guidance, mentorship, and expertise that made this senior capstone possible.

References

- [1] S. Nakai and K. Mima, “Laser driven inertial fusion energy: present and prospective,” *Rep. Prog. Phys.*, vol. 67, no. 3, pp. 321–349, Mar. 2004, doi: 10.1088/0034-4885/67/3/r04.
- [2] E. I. Moses, “Ignition on the National Ignition Facility: a path towards inertial fusion energy,” *Nucl. Fusion*, vol. 49, no. 10, p. 104022, Oct. 2009, doi: 10.1088/0029-5515/49/10/104022.
- [3] H. Abu-Shawareb *et al.*, “Lawson Criterion for Ignition Exceeded in an Inertial Fusion Experiment,” *Phys. Rev. Lett.*, vol. 129, no. 7, Aug. 2022, doi: 10.1103/physrevlett.129.075001.
- [4] H. Abu-Shawareb *et al.*, “Achievement of Target Gain Larger than Unity in an Inertial Fusion Experiment,” *Phys. Rev. Lett.*, vol. 132, no. 6, Feb. 2024, doi: 10.1103/physrevlett.132.065102.
- [5] “UC San Diego joins General Atomics-led fusion collaborative.” Accessed: May 23, 2025. [Online]. Available: <https://www.ans.org/news/2025-02-12/article-6756/uc-san-diego-joins-general-atomicsled-fusion-collaborative/>
- [6] “First Light Fusion | Enabling Inertial Fusion Energy | Our Machines,” First Light Fusion. Accessed: Jun. 08, 2025. [Online]. Available: <https://firstlightfusion.com/our-technology/our-machines/>
- [7] R. W. Petzoldt and R. W. and Moir, “Target Injection Methods for Inertial Fusion Energy,” *Fusion Technol.*, vol. 26, no. 3P2, pp. 896–905, Nov. 1994, doi: 10.13182/FST94-A40268.
- [8] “Approach,” Xcimer Energy. Accessed: Jun. 08, 2025. [Online]. Available: <https://xcimer.energy/approach/>
- [9] D. T. Goodin *et al.*, “A cost-effective target supply for inertial fusion energy,” *Nucl. Fusion*, vol. 44, no. 12, pp. S254–S265, Dec. 2004, doi: 10.1088/0029-5515/44/12/S17.
- [10] M. H. Hablanian, *High-Vacuum Technology: A Practical Guide, Second Edition*, 2nd ed. New York: Routledge, 2017. doi: 10.1201/9780203751923.
- [11] L. Al-Ghussain, “Global warming: review on driving forces and mitigation,” *Environ. Prog. Sustain. Energy*, vol. 38, no. 1, pp. 13–21, 2019, doi: 10.1002/ep.13041.

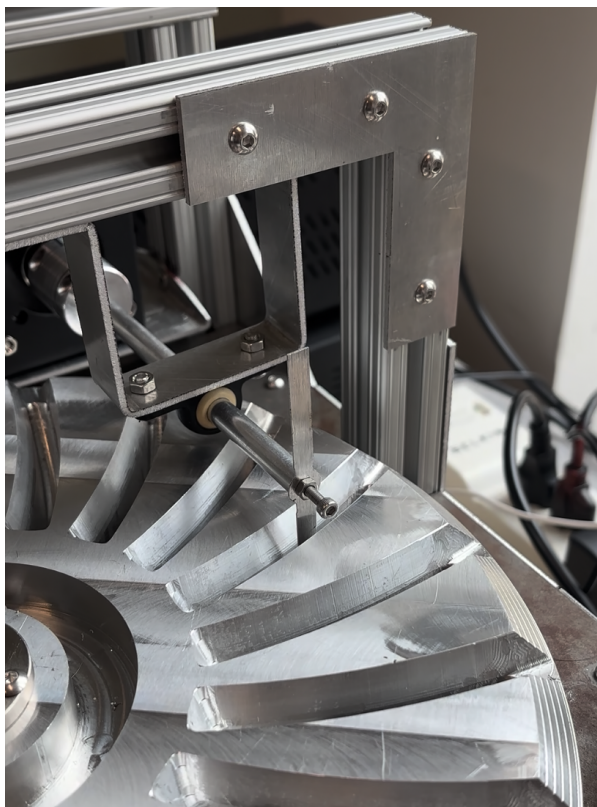
Appendix A: User Manual

First-Time Instructions:

- 1) Install the Arduino IDE. Distributions may be found at this link:
<https://www.arduino.cc/en/software/> for Windows/Mac/Linux operating systems.
- 2) Open Arduino IDE and navigate to the Library tab. Install the “AccelStepper” Library by Mike McCauley. This is used to control the stepper motors.

System Calibration:

- 1) With the system powered off, rotate the ejection arm to point within the bottom-most point of the closest fueling rotor groove. It should look like this:



- 2) With the system still off, open the control box lid and ensure that all electrical connections within the control box are interfaced correctly, and that there are no terminals or exposed wires touching.
 - a) Make sure that the motor terminal is connected to the 24VDC supply, the solenoid terminal to the 12VDC supply, and the Arduino barrel-jack to the 12V wall-wart adapter.
- 3) Close the lid of the control box.
- 4) Power the system by turning on both power supplies.
 - a) The motors have a green LED that should blink when powered
- 5) Connect a computer to the Arduino via USB-C.
- 6) Open Arduino IDE and open the script Named “Full_Stage_Control.ino”
- 7) Navigate to the “Tools” tab, select “Arduino UNO” as the board, and connect the serial port.
- 8) At the top-left corner of the Arduino IDE, first verify and compile the control script by pressing the check-mark button, then upload the script.
- 9) After the script successfully uploads, open the serial monitor by clicking the magnifying glass icon in the upper right corner.
- 10) Follow the next instructions to operate the system:

System Operation:

A switch case with several commandlets allows you to control the speed of the motors and the ejection frequency of the gating system solenoid. Before inputting any targets, in the Serial Monitor:

- 1) To control the stepper motor speeds, write “AX” with “X” being the speed in steps/sec.
IMPORTANT: “X” sets the speed of the fueling rotor; the ejection arm is computed automatically as ten times “X.” You can verify the number of steps per revolution by observing the switch table on each motor that sets the number of steps per revolution. Currently both are set to 400 steps per revolution.

- a) Example Use: Write “A30” sets the fueling rotor speed to 30 steps/sec and the ejection arm to 300 steps/sec.
- 2) To control the solenoid ejection frequency, write “SY,” where “Y” is the frequency in Hz.
- 3) It will be necessary to iteratively tune the fueling rotor speeds with the solenoid ejection frequency until they are in phase. The easiest way is to set a fueling stage speed, and tweak the solenoid frequency until the thrust of the solenoid shaft both lines up with a groove and matches in frequency.
 - a) A20 and S0.25 were found to work well.
- 4) Once you are satisfied with the timing of the system, slowly pour in a batch of targets.
Make sure the sheet metal lid is placed on top of the gating system channel.
- 5) You can optionally save the your speeds to the Arduino’s EEPROM by writing “W”
- 6) Note that all commands must be entered individually, you cannot write multiple in a single line.

System Ramp-Down:

To turn off the system:

In the Serial Monitor:

- 1) Set the Solenoid frequency to 0 Hz by writing “S0”
- 2) Next, set the motor speeds to 0 steps/sec by writing “A0”
- 3) Turn of the power power supplies

In an emergency, the system can be immediately stopped by unplugging the power strip connected to the power supplies and Arduino.

Appendix B: Fabrication Instructions for Additional Units

This appendix outlines how to replicate our current prototype of the IFE target autoloader. Everything listed here is based on what we actually built and tested. We've organized it by subsystem for clarity. Where possible, we used off-the-shelf parts, and any custom components are noted.

1. Target Loading Funnel Assembly

- **Funnel:** We used a standard tin metal funnel from McMaster-Carr with 4.5" height and $\frac{3}{8}$ " spout outer diameter.
- **Stopper:** To prevent jamming at the funnel's outlet, we added a V-shaped sheet metal piece, bent by hand and press-fitted over the opening. This helped center the targets better during loading.
- **Stand:** The funnel stands vertically on a 120 mm T-slot aluminum extrusion (McMaster 47065T101), bolted to a small custom base plate we machined for stability.
- **Tubing:** Flexible PVC tubing (6 mm inner diameter) runs from the funnel down to the gate system. Near the gate, we switch to aluminum tubing (\sim 5.5 mm outer diameter) for better fit and rigidity. This tubing is held in place using a basic U-bracket..

2. Gate System

- **Material:** The gate block is machined from a single piece of Aluminum 6061 stock. We angled the feed path at 7.5° based on trial-and-error testing as it gave us the smoothest flow without bouncing.
- **Solenoid:** The actuator is a push-pull solenoid from Amazon (model DS-0420S). It operates on 12V, has a 5 mm stroke, and can exert around 5N of force, enough for lightweight targets.
- **Mounting:** The gate is mounted on a 295 mm T-slot rail using a custom aluminum plate (150 mm \times 200 mm, 5 mm thick). We bent the plate edges to allow for some height adjustment on the T-slots without redesigning the whole structure.

- **Fastening:** Everything is bolted down with M3 hardware. The aluminum tubing feeding into the gate is clamped using a U-bracket directly on the gate body.

3. Rotary Fueling Disk Assembly

- **Rotor:** This part was CNC'd from Aluminum 6061 using a HAAS VF2 at our machine shop. It includes spiral grooves for target holding.
- **Base Plate:** The rotor is mounted on a flat 2 mm thick steel plate (314 mm × 354 mm), supported underneath by four 175 mm long T-slot rails. This gives enough rigidity and spacing for the motor and shaft setup.
- **Shaft:** We used an 8 mm stainless steel shaft (from McMaster), supported with standard adjustable bearing inserted into the upper T-slot frame.
- **Motor:** A NEMA 17 stepper motor (McMaster 6627T122) is used to drive the rotor. It's connected using a standard shaft coupler.

4. Ejection Arm

- **Material:** The ejection arm is made from 1 mm thick aluminum, laser-cut and manually bent. We experimented with several designs and the one we used has twisted ends that taper to about 5.75 mm, providing a 0.25 mm clearance inside the rotor grooves.
- **Shaft:** This uses a 5 mm stainless steel shaft (also from McMaster). The ejection arm is held in place with a single M2 tapped hole and screw.
- **Motor:** It's driven by a second NEMA 17 stepper motor, again with a shaft coupler. Both motors run independently in the current version.

5. Control Electronics

- **Controller:** We used an Arduino Uno to control the motors and solenoid. The speed of the two motors are related by an equation in the code.
- Power Supply:** A standard 12V DC bench power supply powers the entire setup.
- **Connections:** Everything is wired on a breadboard using jumper cables for prototyping.

Appendix C: Technical Drawings

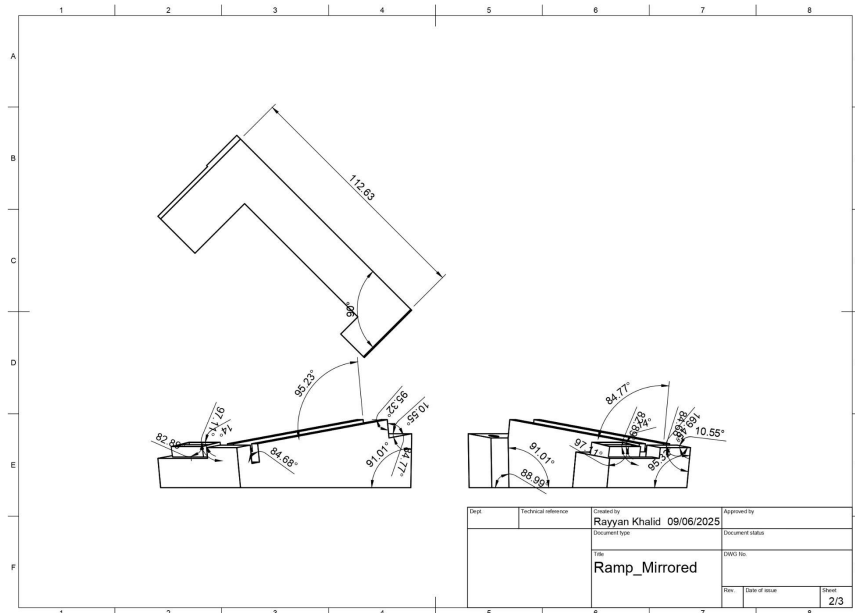
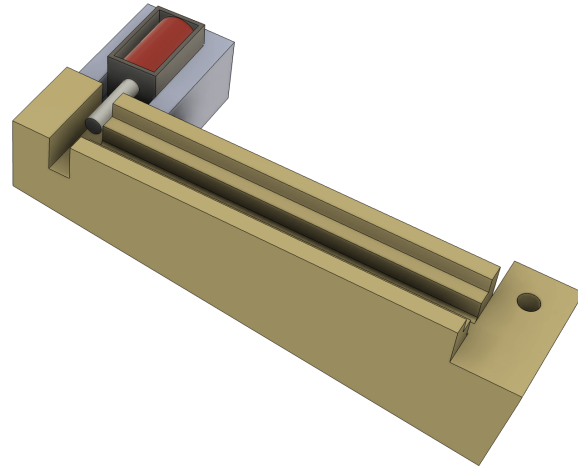
All drawings and CAD files can be found on our team website, linked here:

Funnel system:



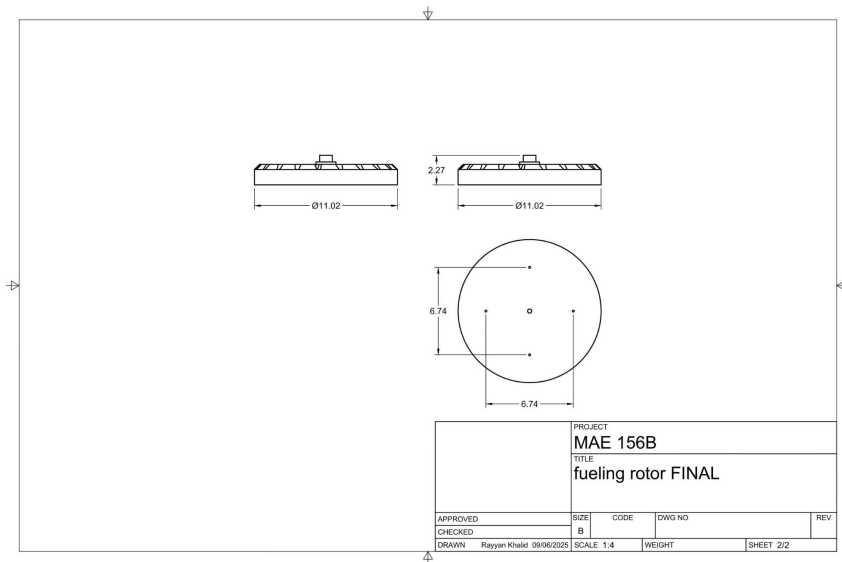
<https://drive.google.com/file/d/116OIN1B34HbENUxzozf8t3Uz5r3p5IhA/view?usp=sharing>

Gate System:



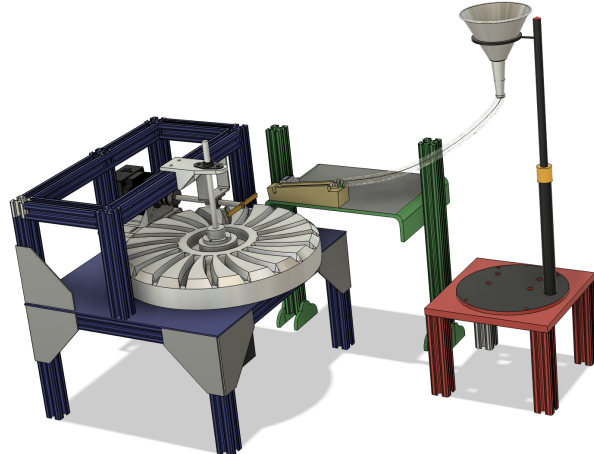
<https://drive.google.com/file/d/1nYCP84KEyp6xZtekdkoFPiebXlfTT4xu/view?usp=sharing>

Fueling Rotor:



<https://drive.google.com/file/d/1ko0GfVPDHUbezT8hMThiPsdNN2O3fgdL/view?usp=sharing>

Full Assembly:



<https://drive.google.com/file/d/1q3QFQN8aA8f8URxpcBv1nMsX2yR861OK/view?usp=sharing>

Link to the Code used for electronics:

<https://drive.google.com/file/d/1Ag7gM2KTHHAB1KxqndSiXtPAcz0hBwnL/view?usp=sharing>

Old Rotary disk:

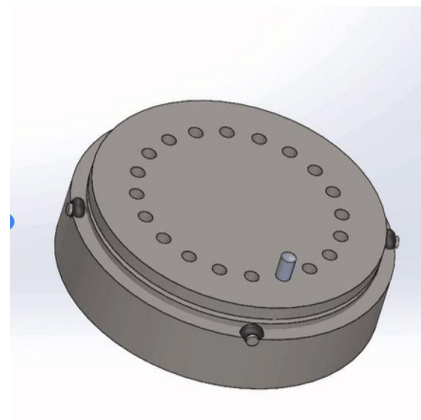


Figure C1: Old design of the rotary disk

All files and CAD can be found here as well:

<https://github.com/Haruncodes/Fusion-Energy-Project-MAE-156B-SP25>

Appendix D: Analytical Methods

Rotor Groove Profile Derivation:

The fueling stage of the Autoloader relies on precise synchronization between the fueling rotor and ejection arms. The fueling rotor is designed to allow the ejection arm arm to pass through the slot as they are both moving without interfering with the side walls of the fueling grooves. The groove geometry that would allow this can be found via kinematics as follows:

Firstly, assume that the rotor and ejection arm are spinning at constant angular velocities ω_1 , ω_2 , respectively. Let R_1 be the radius of the fueling rotor, and R_2 be the radius of the arc that a single ejection arm traces. The ejection arm spins perpendicularly with respect to the fueling rotor, and collinear with its radial direction at a radial offset in the plane of C in the x-direction. This model is shown in Figure D1.1.

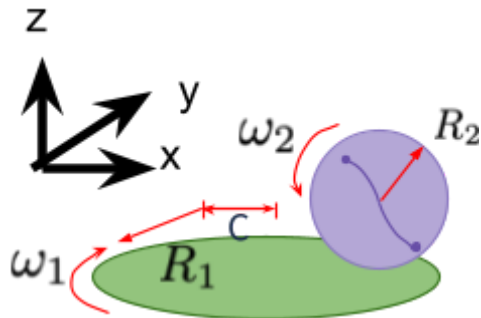


Figure D1.1: Kinematic diagram of the fueling stage.

The velocity of the tip of the ejection arm is given by $v_2 = R_2 \omega_2$. In the stationary frame of the fueling rotor, it can be shown that the tip of the ejection arm shaft would follow the trace given by the set of parametric equations

$$x = (v_2 t + C) \cos \omega_1 t \quad (\text{Eq. D1.1})$$

$$y = (v_2 t + C) \sin \omega_1 t \quad (\text{Eq. D1.2})$$

Conversion from cartesian to polar coordinates, yields

$$\begin{aligned} \sqrt{x^2 + y^2} &= \frac{v_2}{\omega_1} \arctan\left(\frac{y}{x}\right) + C \\ \Rightarrow r &= \frac{v_2}{\omega_1} \theta + C, \\ r &= \frac{R_2 \omega_2}{\omega_1} \theta + C = R_2 N \theta + C, N = \omega_2 / \omega_1. \quad (\text{Eq. D1.2}) \end{aligned}$$

Equation D1.2 therefore describes the projection of the ejection arm arm as it passes through the fueling rotor in polar coordinates, where:

- N = the ratio of the angular speed of the ejection arm arm to the fueling rotor,
- R_2 = radius of the ejection arm arm
- C = the radial offset of the ejection arm to the center of the fueling rotor.
- r = the distance from the origin to a point on the ejection arm arm as it passes through the rotor

Since there are 20 grooves in the fueling rotor, and there are two ejection arms, the two ejection arms must spin ten times as fast as the fueling rotor, thus $N = 10$. This relationship informed the spiral groove geometry in the fueling rotor, ensuring that the ejection arm passes through each groove smoothly. The groove shape is thus scalable, allowing the system to support shot rates beyond the 0.25 Hz minimum by simply increasing rotational speed while maintaining the ratio.

Appendix E: Budget

| Expense details | Cost | Transaction date | Paid by | Notes | Budget left |
|-----------------|------------|------------------|---------|------------------|-------------|
| Shared Shop | \$1,800.00 | | | Paid directly to | \$6,200.00 |

| Expenses | | | | school by sponsor | |
|--|----------|-----------|----------|---|------------|
| Spherical Targets | \$9.50 | 3/10/2025 | Rayya... | ASG Blaster Airgun Plastic BB, 4.5mm, 0.13g - 1000 pcs. | \$6,190.50 |
| Motors | \$9.68 | 3/10/2025 | Rayya... | Gikfun 1.5V-6V Type 130 Miniature DC Motors for Arduino Hobby Projects DIY (Case Pack of 6) EK1450 | \$6,180.82 |
| Motor Driver Controller Board Module Stepper Motor | \$11.49 | 3/10/2025 | Rayya... | HiLetgo 4pcs L298N Motor Driver Controller Board Module Stepper Motor DC Dual H-Bridge for Arduino Smart Car Power UNO MEGA R3 Mega2560 | \$6,169.33 |
| Battery Holder Leads | \$6.49 | 3/10/2025 | Rayya... | LAMPVPATH 3 Pcs 4 x 1.5V (6V) AA Battery Holder Leads with 3 Pcs 9V I Type Snap Connector Plastic Housing Two Layers Battery Case | \$6,162.84 |
| 2 wheels | \$17.70 | 3/15/2025 | Rayya... | https://www.mcmaster.com/product/9960T663 | \$6,145.14 |
| Vibra 6" Mini Vibratory Bowl Feeder | \$184.00 | 4/28/2025 | Mae ... | https://www.ebay.com/item/126200381851 | \$5,961.14 |
| 12" Aluminum 6061 Disk stock 2" thick | \$312.56 | 4/29/2025 | Mae ... | https://www.mcmaster.com/products/aluminum/alu-minum-2~/multipurpose-6061-aluminum-rods-and-disks-7/shape~disc/material~6061-alumin/ | \$5,648.58 |

| | | | | | |
|---|---------|-----------|----------|---|------------|
| T-Slotted Framing Rails 10ft | \$47.35 | 4/30/2025 | Mae ... | https://www.mcmaster.com/products/t-slotted-framing/t-slotted-framing-and-fittings~/t-slotted-framing-rail-s-4/ | \$5,601.23 |
| High-Speed Steel Tapered Square End | \$38.42 | 5/1/2025 | Mae ... | https://www.mcmaster.com/8936A88 | \$5,562.81 |
| 2PCS Mini Push Pull Linear Solenoid | \$17.23 | 5/2/2025 | Ravi ... | https://www.amazon.com/Solenoid-Electromagnet-Actuator-Electric-DS-0420S/dp/B0BMVDPWS3/ref=sr_1_3?crid=1039L3MRVIUQ8&dib=eyJ2IjoiMSJ9.iMrjwDmWIDAqu-nOpxnLGUHo2ZcDdhN0cxH9j0bYdV0vRgz5NKK_WsCD0YK6uph5bqDwbTCHeMslqRc0awd6tz3KJYgYf7k8z20SYda5Qf_tC6TO-pRhqptHa3q51TpN0H_RiUfnYuJsyZMqYc7sDN8HpJKWf7S9aAuJll1XNkaWCr9JQJe6tgzeLXswTiuby70pzW3eaGCb-kMsedes-BZs9jjcYxj7VQC5MVp27o.sIB4K-rPUivwKjb_oAcn076qMGOTIzpZiKtri01cYUkw&dib_tag=se&keywords=12v+push+pull+solenoid+5mm&qid=1745613192&sprefix=12v+push+pull+solenoid+5mm%2Caps%2C172&sr=8-3 | \$5,545.58 |

| | | | | | |
|---|---------|----------|---------|---|------------|
| Uncoated High-Speed Steel Tapered Square End Mil | \$31.88 | 5/2/2025 | Mae ... | https://www.mcmaster.com/8936A971 | \$5,530.93 |
| Corrosion-Resistant Timing Belt Pulley, XL Series, 3/8" | \$55.71 | 5/2/2025 | Mae ... | https://www.mcmaster.com/1277N31 | \$5,475.22 |
| Corrosion-Resistant Timing Belt Pulley, XL Series, for 3/8" | \$11.77 | 5/2/2025 | Mae ... | https://www.mcmaster.com/1277N45 | \$5,463.45 |
| XL Series Timing Belt, Trade No. 170xL037 | \$11.18 | 5/2/2025 | Mae ... | https://www.mcmaster.com/6484K227 | \$5,452.27 |
| Timing Belt, XL Series, 3/8" wide | \$10.58 | 5/2/2025 | Mae ... | https://www.mcmaster.com/6484K837 | \$5,441.69 |
| Metal Bevel Gear, 10 mm Face Width, 1.5 Module, 3:1 Speed Ratio | \$64.18 | 5/2/2025 | Mae ... | https://www.mcmaster.com/2515N328 | \$5,377.51 |
| Metal Pinion, 10mm Wide Face, 1.5 Module, 3:1 | \$25.03 | 5/2/2025 | Mae ... | https://www.mcmaster.com/2515N319 | \$5,352.48 |
| Funnel Stand Filter Holder | \$14.99 | 5/2/2025 | Mae ... | https://www.amazon.com/FUNGDO-Holder-Adjustable-Photosensitive-Only/dp/B0D3BQH4GF?gQT=1&th=1 | \$5,337.49 |
| 5 FL oz Tin Funnel 2" spout 3/8" OD | \$6.99 | 5/2/2025 | Mae ... | https://www.mcmaster.com/8996T12 | \$5,330.50 |
| Aluminum Tubing | \$7.75 | 5/2/2025 | Mae ... | https://www.mcmaster.com/89965K341 | \$5,322.75 |
| PVC Tubing | \$13.40 | 5/2/2025 | Mae ... | https://www.mcmaster.com/5233K126 | \$5,309.35 |
| 30W Concrete Vibrator Motor | \$49.00 | 5/2/2025 | Mae ... | https://www.amazon.com/XINJIAHONG-Concrete-Vibrator-Vibration-Vibration/dp/B0DJ54Y437/ref=sr_1_12 | \$5,260.35 |

| | | | | | |
|---|----------|-----------|---------|---|------------|
| | | | | ?crid=2Q9EZGYDZ904E&dib=eyJ2ljoiMSJ9.P3MUxKn5PGcDYK3Hc4TB4eyJB03tdrFIHz1vRqvxqQ13webAZNa1mtKS02RHCOqftoeNFZuiBULWJRxcEJjUBIQu4095wBgsdhWL7ut6MAGE82okdkdB-aALsBHeNbOjY0tiGkAHubybkYepIJn0t7iKB04Q0VjQlzlOXnlK9jekRCxYLkkjtQfNn62W9cIHNDiXMzAJIQq9_Euw436tGjicu96ckhRWc97vCgmm3L_UhZsyfVK_yvSZDKhppffDqiSBoc16Clcz4TD7sba44Q&dib_tag=se&keywords=vibrating+motor&qid=1746215056&sprefix=vibrating+motor%2Cspecialty-aps%2C191&sr=8-12 | |
| Tax + Shipping | \$56.70 | 5/2/2025 | Mae ... | For some of the above stuff | \$5,203.65 |
| Stepper Motor Mounting Bracket ST-M2 | \$8.48 | 5/13/2025 | Mae ... | https://www.amazon.com/gp/product/B00Q6GI05K?asin=B00Q6GI05K&tag=eyJ2ljoiMSJ9.P3MUxKn5PGcDYK3Hc4TB4eyJB03tdrFIHz1vRqvxqQ13webAZNa1mtKS02RHCOqftoeNFZuiBULWJRxcEJjUBIQu4095wBgsdhWL7ut6MAGE82okdkdB-aALsBHeNbOjY0tiGkAHubybkYepIJn0t7iKB04Q0VjQlzlOXnlK9jekRCxYLkkjtQfNn62W9cIHNDiXMzAJIQq9_Euw436tGjicu96ckhRWc97vCgmm3L_UhZsyfVK_yvSZDKhppffDqiSBoc16Clcz4TD7sba44Q&dib_tag=se&keywords=vibrating+motor&qid=1746215056&sprefix=vibrating+motor%2Cspecialty-aps%2C191&sr=8-12 | \$5,195.17 |
| Three 5ft length T-Slotted Framing, Single Four Slot Rail, Silver, 1" High x 1" Wide, Solid | \$86.79 | 5/13/2025 | Mae ... | 47065T101 | \$5,108.38 |
| Stepper Motor with Integrated Motion Control, NEMA 23, 76 in.-oz. Maximum | \$221.67 | 5/13/2025 | Mae ... | 6627T122 | \$4,886.71 |

| | | | | | |
|--|----------|-----------|----------|---|------------|
| Clamping Precision Flexible Shaft Coupling, Spiral, 7075 Aluminum, for 8mm x 1/4" Shaft Diameter, 30mm Long | \$69.05 | 5/13/2025 | Mae ... | 2464K19 | \$4,817.66 |
| Clamping Precision Flexible Shaft Coupling, Spiral, 7075 Aluminum, for 8mm x 8mm Shaft Diameter, 30mm Long | \$69.05 | 5/13/2025 | Mae ... | 2463K28 | \$4,748.61 |
| Dry-Running Mounted Sleeve Bearing for Extreme Misalignment, for 8 mm Shaft Diameter | \$10.76 | 5/13/2025 | Mae ... | 6687K33 | \$4,737.85 |
| Mounted Ball Bearing with Two-Bolt Flange, Two-Bolt Flange, Chrome-Plated Bearing, for 8 mm Shaft Diameter | \$14.07 | 5/13/2025 | Mae ... | 4473N18 | \$4,723.78 |
| Clamping Two-Piece Shaft Collar for 8 mm Diameter, Black-Oxide 1215 Carbon Steel | \$39.72 | 5/13/2025 | Mae ... | 6063K14 | \$4,684.06 |
| 6x6" Multipurpose 6061 Aluminum Sheet, 1-1/2" Thick | \$74.40 | 5/13/2025 | Mae ... | 89155K18 | \$4,609.66 |
| Tax + Shipping | \$75.42 | 5/13/2025 | Mae ... | For above McMaster stuff | \$4,534.24 |
| Home Depot Run | \$120.35 | 5/26/2025 | Colby... | | \$4,413.89 |
| DC Power Supply Variable | \$51.15 | 5/27/2025 | Mae ... | https://www.amazon.com/gp/product/B09BFCF13Y/ref=ox_sc_act_title | \$4,362.74 |

| | | | | | |
|---|----------|-----------|---------|---|------------|
| | | | | https://www.amazon.com/gp/product/B00TP1C51M/ref=ox_sc_act_title_1?smid=A306VK2RLCY3C4&th=1 | |
| Amazon Basics 6-Outlet Surge Protector | \$11.59 | 5/27/2025 | Mae ... | https://www.amazon.com/gp/product/B09BFCF13Y/ref=ox_sc_act_title_2?smid=A306VK2RLCY3C4&th=1 | \$4,351.15 |
| DC Power Supply Variable | \$52.79 | 6/6/2025 | Mae ... | https://www.mcmaster.com/catalog/131/1315/6627T122 | \$4,298.36 |
| Stepper Motor with Integrated Motion Control, NEMA 23, 76 in.-oz. Maximum | \$248.01 | 6/6/2025 | Mae ... | https://www.mcmaster.com/catalog/131/1315/6627T122 | \$4,050.35 |

Appendix F: Project Management

F.1: Task Distribution

- Sponsor Liaison: Tanmay Prakash
- Webmaster: Julian Ramirez
- Document Coordinator: Ravi Harun
- Fiscal and Schedule Coordinator: Rayyan Khalid
- Safety Coordinator: Colby Hettinger

F.2: Intermediate Milestones

- Initial design of rotary system: 02/18/2025
- Prototyped initial design for risk reduction: 02/27/2025
- Performed risk reduction testing: 03/18/2025
- Identified issues in the original design: 03/20/2025
- Finalized the design for rotary system: 04/08/2025

- Finalized system for targets intake: 04/24/2025
- Finalized design for gate system: 05/01/2025
- Manufactured the rotary disk: 05/16/2025
- Manufactured the gate system: 05/20/2025
- Integrated all systems together: 05/23/2025

F.3: Risk Reduction Efforts

Ejection Arm Interference and Misalignment

Identified Risk: The Ejection Arm risked colliding with the rotary disk if misaligned or started from an incorrect rotational position. Additionally, improper timing could cause scooping issues for the targets.

Mitigation Strategy:

To address this, the team implemented strict geometric tolerances between the ejection arm and the spiral grooves of the disk. Manual alignment protocols were followed during every test cycle to ensure safe starting orientation. Future design recommendations include adding an encoder to the ejection arm shaft to guarantee consistent starting position and improve integration with feedback control.

Funnel and Gate Jamming

Identified Risk: High potential for targets to jam at the funnel outlet or within the feed tube, especially under bulk loading conditions. Jamming could result in inconsistent delivery, overflow into the gate, or multiple targets reaching the solenoid.

Mitigation Strategy:

A custom V-shaped stopper was designed and press-fit onto the funnel outlet to limit target pileup at the throat of the funnel. The gate system was revised from a two-gate to a single-push solenoid design, eliminating the risk of backflow and target crushing during gate closure. Bench

tests validated the effectiveness of this configuration with zero observed jams across repeated runs given that targets are poured in slowly.

F.4: Lessons Learned

- Several machined and ordered parts had longer-than-expected lead times; finalizing critical designs earlier in MAE 156B helped avoid last-minute delays.
- Modular, adjustable design (e.g., T-slot frames) made iterative testing and part replacement easier.
- Clear division of roles and regular weekly check-ins improved team coordination and progress tracking.
- Earlier testing of actuation timing (solenoid and ejection arm) would have revealed integration issues sooner.
- In future iterations, integrating sensors and feedback loops early in the process would enhance system robustness and reduce manual dependency.

F.5: Individual Component Analysis

F.5.1: Ravi Harun - Machining, Manufacturing and Fabrication

<https://drive.google.com/file/d/10a29muMDvJWv9lLKWpr-yMXAPrOeTl5g/view?usp=sharing>

F.5.2: Tanmay Prakash - Failure Prevention Analysis and IFE Target Simulations

<https://drive.google.com/file/d/1gZdiXdnmesTRiUqtB68exAJDWYlbAmix/view?usp=sharing>

F.5.3: Colby Hettinger - Material Selection

<https://drive.google.com/file/d/10a29muMDvJWv9lLKWpr-yMXAPrOeTl5g/view?usp=sharing>

F.5.4: Rayyan Khalid - CAD Design and Animation of the Rotary system

<https://drive.google.com/file/d/1eXYeSUVSz06KriwVS3m0KPLarji0ynsy/view?usp=sharing>

F.5.5: Julian Ramirez - Rotational Actuator Integration

https://drive.google.com/file/d/1porvwYocS_sVLtOHa93RI7VdtONItMUI/view?usp=sharing

Appendix G: Executive Summary

Fusion energy is an emerging technology with immense promise as a future power source to meet rising global energy demands. It is a nuclear process by which two light atomic nuclei combine to form a heavier nucleus, releasing substantial amounts of energy in the process. Unlike fossil fuels, fusion relies on abundant resources like hydrogen, and does not emit greenhouse gases [1]. Furthermore, fusion does not produce the same long-lived radioactive waste associated with conventional nuclear fission power and carries no risk of catastrophic meltdowns. One way to achieve fusion is through the inertial confinement scheme, where a small fuel-filled spherical target is imploded using lasers [2]. This was the scheme that, for the first time ever, net energy was released from a fusion process in 2022 [3]. With this precedent set, a growing initiative is underway to explore how we can leverage this reaction to produce energy at the power-plant level.

Extreme conditions are necessary to enable inertial fusion to be viable as a commercial power source that demand novel engineering solutions, including the requirement that targets be shot at least ten times per second continuously. To this end, we have been sponsored through a collaboration between the UCSD Fusion Engineering Institute, and the General Atomics Fusion Energy Program to develop a system that automates preparation of fusion targets for deployment into a reactor, called the Autoloader.

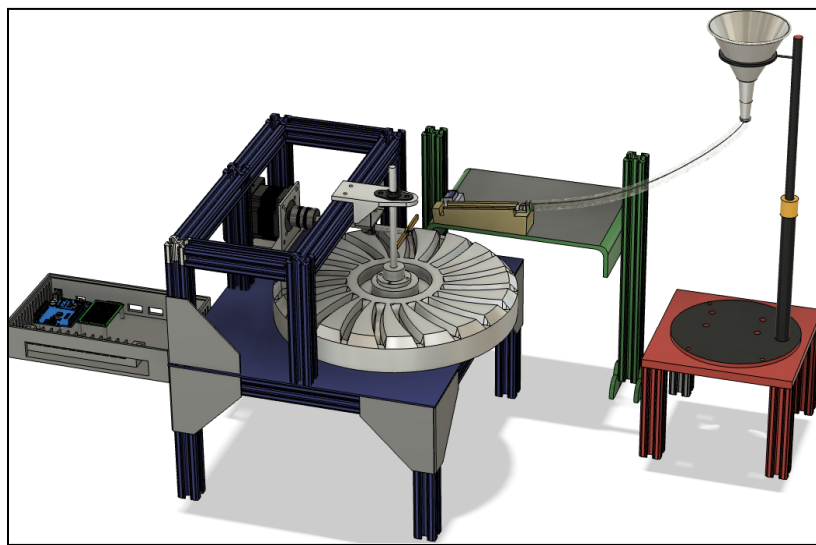


Figure G.1: CAD of Autoloader Device.

As seen in Figure G.1, the Autoloader consists of four main components: the input funnel (shown in red), the gating system (green), the fueling stage (blue), and the controller (gray). A batch of target shells is poured into the funnel, and gravity fed to the gate system. A push-pull solenoid dispenses the shells individually into grooves of the large circular fueling rotor, where the shells can be doped with liquid hydrogen fuel. A small ejection arm removes the doped targets from the grooves towards the next assembly in the reactor.

Testing has shown that the Autoloader is capable of dispensing prepared targets at a minimum shot rate of 0.25 Hz, and can scale to higher shot rates with 90% accuracy. The Autoloader is designed to be quickly outfitted for use in vacuum and cryogenic conditions by using metal construction and parts with close cryogenic analogs like ceramic bearings. Figure G.2 shows the final system prototype.



Figure G.2: The Final Autoloader Assembly

[1] R. L. Hirsch and W. L. R. Rice, “Nuclear Fusion Power and the Environment,” *Environ. Conserv.*, vol. 1, no. 4, pp. 251–262, 1974, doi: 10.1017/S0376892900004823.

- [2] S. Nakai and K. Mima, “Laser driven inertial fusion energy: present and prospective,” *Rep. Prog. Phys.*, vol. 67, no. 3, pp. 321–349, Mar. 2004, doi: 10.1088/0034-4885/67/3/r04.\
- [3] E. I. Moses, “Ignition on the National Ignition Facility: a path towards inertial fusion energy,” *Nucl. Fusion*, vol. 49, no. 10, p. 104022, Oct. 2009, doi: 10.1088/0029-5515/49/10/104022.